energies

MDPI

Article

Feasibility Study of a Hybrid Building High Voltage Alternating Current and Domestic Hot Water System Combining a Photovoltaic-Thermal System and a Ground Source Heat Pump

Yong-Dae Jeong [1], Min Gyung Yu [2] and Yujin Nam [2,*]

[1] Building Energy Technology Center & Center for Climatic Environment Real-Scale Testing, 7 Jeongtong-ro, Deoksan-myeon, Jincheon-gun, Chungcheongbuk-do 27872, Korea; jyd2092@naver.com

[2] Department of Architectural Engineering, Pusan National University, 2 Busandaehak-ro 63, Geomjeong-gu, Busan 46241, Korea; min324806@gmail.com

* Correspondence: namyujin@pusan.ac.kr; Tel.: +82-51-510-7652; Fax: +82-51-514-2230

Received: 8 June 2017; Accepted: 17 August 2017; Published: 21 August 2017

Abstract: Renewable energy systems have received a lot of attention as sustainable technology in building sector. However, the efficiency of the renewable energy systems depends on the surrounding conditions, and it could gradually decrease by excessive and long-term operation. As a solution, a hybrid system can increase the reliability of energy production and decrease investment costs through by reducing the system capacity. The hybrid system operates at the ideal performance, but the design and operation method for hybrid system have not been established. In this paper, the performance of the hybrid system combined with photovoltaic/thermal (PVT) system and ground source heat pump (GSHP) system was analyzed using TRNSYS 17 and feasibility was assessed. The energy consumption and performance efficiency of hybrid system were calculated according to operating modes. Furthermore, seasonal performance factor (SPF) of hybrid system was compared with that of conventional GSHP system. System performance was analyzed in various conditions such as the usage of storage tank heating and set temperature for solar heating. As a result, the average SPF of the developed system increased about 55.3% compared with the GSHP system.

Keywords: hybrid system; photovoltaic/thermal; ground source heat pump system; performance analysis

1. Introduction

Recently, renewable energy system represent a sustainable and energy-saving technology in buildings. In Korea, solar-energy systems such as photovoltaic (PV) have been regarded as the most popular among the renewable energy systems. As for solar energy, it is expected to have considerable potential as a main energy source in the future. The energy-generation efficiency of the PV system, however, depends on the local solar radiation and the surrounding conditions, and it gradually decreases as a result of the warmed surface temperature of the solar panel; furthermore, the photovoltaic cells have significantly expensive installation costs [1–3]. A PVT system, which is devised to increase the efficiency of the PV system, extracts heat from the PV module through air or liquid, and it is classified according to the types of heating media and glass cover. An unglazed PVT collector consists mainly of the heat-removal pipes located on the backside of the PV module, which reduce the temperature of the PV module. An additional glass cover can increase the thermal performance of the collector though, it conversely reduces slightly the optical and PV performances of the module [4,5]. A water-type PVT system would be definitely advantageous to save space and increase the efficiency of the heat exchange rate [6].

Another renewable energy system, the ground source heat pump (GSHP) system, is on the rise as an efficient technology for space heating and cooling in buildings. It can achieve high energy-savings by utilizing annually stable underground temperatures as a heat source. The system performance depends on the underground conditions such as ground thermal conductivity, underground temperature, and groundwater level. However, excessive or long-term operations could lead to the decrease of system performance for GSHP system. Therefore, several methods with an auxiliary heat source or ground heat exchanger have been studied to prevent reducing the ground temperature. In this research, a hybrid system which consists of a photovoltaic/thermal (PVT) and a geothermal solar-heat pump (GSHP) is suggested to solve this problem.

This hybrid system can enhance the reliability of the energy production and decrease the investment costs by reducing the system capacity. In addition, it is able to recover the underground temperature, and from an energy viewpoint it operates independently by utilizing the electrical and thermal production of the PVT module. Moreover, the PVT system integrated with the GSHP system has other advantages. The surface temperature of the PVT-module would be lower, so that it can increase power-production to further improve the performance efficiency.

Many studies have been carried out on hybrid systems which combine a GSHP system and a solar system. Wang and Qi [7] analyzed the performance of underground thermal storage for a solar ground-coupled heat-pump system (SGCHPS) for a residential building. Based on the experiment results, the system performance during a longer period was simulated according to unit modeling, and its parametric effects were discussed. The results suggested that the performance of the underground thermal storage of the SGCHPS depends strongly on the intensity of the solar radiation and the match between the water-tank volume and the area of the solar collectors. A reasonable ratio between the tank volume and the area of the solar collectors was suggested to be in the range of 20 L/m^2 to 40 L/m^2. An experimental study on a solar-assisted ground-coupled heat-pump system with a solar-seasonal thermal storage installed in a cold-area house was presented by Wang et al. [8]. In this case, the results provided that the system could meet the heating and cooling energy needs of the building with average system performance coefficients of 6.55 and 21.35, respectively. Further, in the heating and cooling modes of the Wang et al.'s [8] study, the operation of the heat pump was not required. Ozgener [9] used a system that comprises a solar-assisted geothermal heat pump and a small wind turbine for the heating in agricultural and residential buildings. Here, the study theoretically showed that 3.13% of the annual electrical-energy consumption of the modeled system and 12.53% of the annual electrical-energy consumption of the secondary water pumping, brine pumping, and fan coil can be met by utilizing the small wind-turbine system (SWTS). This result indicated that the combination of a modeled passive solar-pre-heating technique with the geothermal heat pump system (GHPS) and the SWTS is economically preferable to the conventional space-heating/cooling systems in agricultural and residential building-heating applications; but only if these buildings are installed in regions with sufficient wind resource.

Chen and Yang [10] conducted a numerical simulation of a solar-assisted ground-coupled heat-pump system in northern China to provide both space heating and domestic hot water. The simulation results indicated that the solar-collector area of the optimized system under the specified load conditions is 40 m^2, while the borehole depth is 264 m. Here, the annual total-heat extraction, plus 75% of the hot-water requirement, can be provided by solar energy when the optimized design is used. Wang et al. [11] presented a novel hybrid solar-geothermal solar-heat-pump system (HSGSHPS) that is composed of a ground heat-pump system (GHPS) and a solar-assisted GSHPS (SAGSHPS). The simulated results showed that the design of the proposed HSGSHPS is reasonable to solve the ground-temperature imbalance problem. A suitable control strategy for the solar collector and storage was found according to the performance of the SAGSHPS. In addition, 32% of the electrical-energy consumption in the HSGSHPS could be saved if the load-circulation pump is turned off when none of the fan coils are running. Using the previous experimental investigations, Yang et al. [12] carried out a numerical simulation regarding the performance of an SGSHPS operated in different heating

modes. Accordingly, the heat-pump performance, solar-collection performance, and borehole-wall temperature were analyzed. According to Yang et al.'s [12] experiment results, the system-operation efficiency during the day can be improved with the assistance of solar energy in the combined operation mode, while the excess solar energy collected during the day can be stored at the ground through the ground-heat exchanger to improve the operation performance of the ground-source heat pump (GSHP) during the night.

Solar and ground heat-pump systems were discussed in the International Energy Agency (IEA) Task 44 Annex 38 [13]. A variety of combinations of solar and heat pump systems were presented, and a performance-assessment method was finally suggested [13,14]. Although various previous studies have been performed, a detailed method of system design and operation was not established. Especially, there is few data to help decide a suitable system capacity in response to the building load and local climate conditions. Furthermore, even though many researchers have suggested the feasibility of a hybrid system with solar and geothermal energy, there are few studies on quantitative analysis of system performance for PVT and GSHP systems by transient energy simulation. It is very important for the performance prediction of the hybrid system to analyze it under dynamic load conditions by the integrated simulation because the operation methods of the individual systems components significantly affect the performance of the other components. Therefore, the purpose of this study is to provide basic data for setting optimal design guidelines for a hybrid system that combines a PVT system and GSHP system by analyzing system performance dynamically according to various operation modes. A performance analysis considered the climatic conditions and typical buildings in Korea. In this paper, the seasonal performance factor (SPF) of the combined GSHP–PVT (Geo-PVT) system was studied and its economic feasibility was estimated under various installation conditions such as building load or weather conditions. Furthermore, the efficiency of the hybrid system was improved by analyzing the operation modes between the PVT and the GSHP system. The result was quantitatively compared with the conventional GSHP system, and an effective operation method was suggested.

2. Analysis Model

2.1. System Summary

The main advantage using both the GSHP and PVT is that they are designed to complement one another. In general, GSHP systems require a significant initial cost to dig boreholes and install ground heat exchangers, and the solar system could offset the cost by partially meeting the heating load. Additionally, GSHP system can stabilize heating and cooling energy supply even though the performance of the PVT system differs on weather condition. Plus, the Geo-PVT system can establish an energy-independent building by producing both electricity and thermal energy for heating, cooling and hot water.

Figure 1 shows system concept of Geo-PVT system. The Geo-PVT system consists of a ground-heat exchanger (GHE), a heat pump, a circulation pump in source side (P1), a circulation pump in load side (P2), a PVT module, a solar-circulation pump (P3), a heat-storage tank (HST), a storage-circulation pump (P4), a fan-coil unit (FCU), and three-way valves. Basically, the main load of building is covered by the GSHP system. PVT system and heat storage tank (HST) can be utilized as auxiliary heat source to reduce peak load. In summer season, cooling operation is performed only with the GSHP system. Thermal energy is supplied from both the GSHP and PVT systems to the HST and building, and the thermal energy in the storage tank is used for both heating and hot-water supply. System operation is controlled by the circulation pumps and the three-way valves.

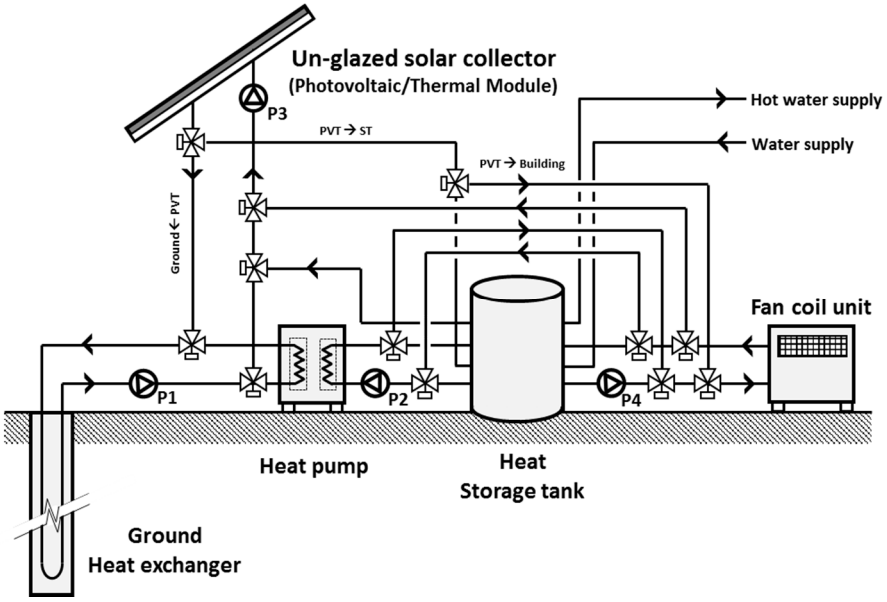

Figure 1. System concept of Geo- photovoltaic/thermal system.

2.2. System Operation Modes

The Geo-PVT system has seven operation modes, as shown in Figure 2, including three heating-operation modes, one cooling mode, two heat storage modes, and an underground heat storage mode. The cooling operation is only performed through the heat pump. Each operation mode of the Geo-PVT system depends on the temperature condition of heat source and the existence of loads. The operation mode can be categorized into the following three types: heating and cooling mode, heat-storage mode, and underground heat-storage mode.

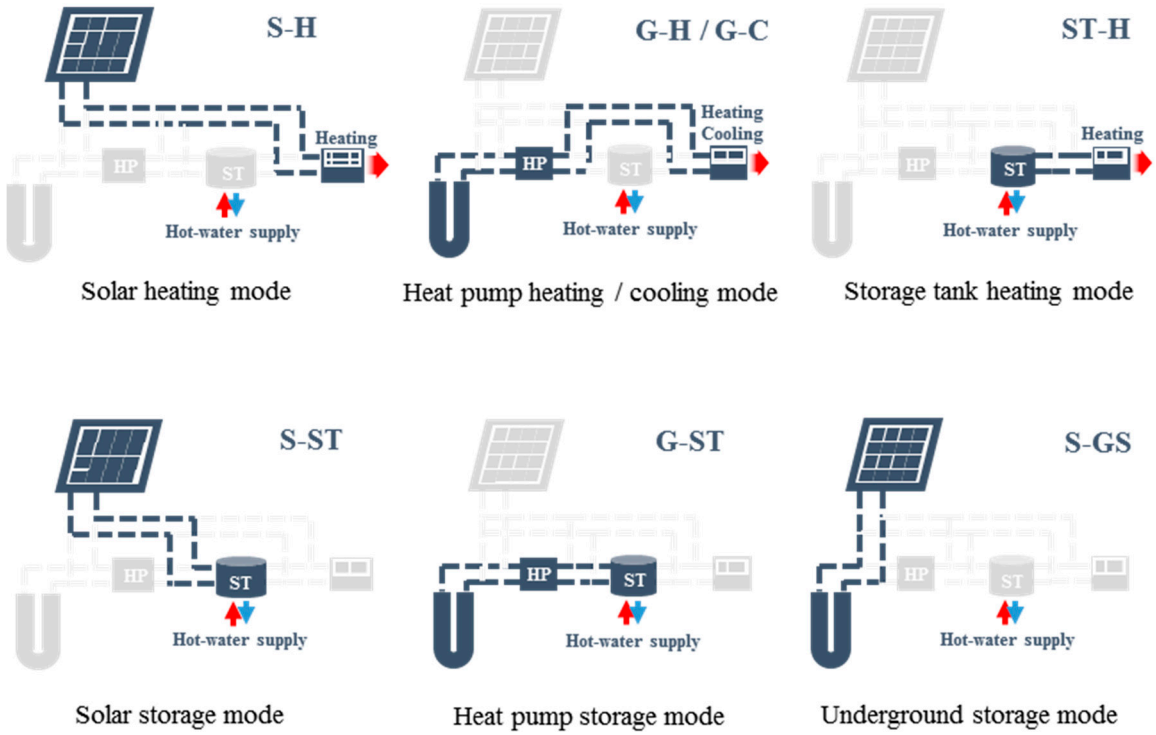

Figure 2. Operation modes of Geo-PVT system.

Figure 3 presents the control algorithm of the system. In this figure, the design temperature of room was set at 22 °C for the heating operation and 26 °C for the cooling operation [15], which can be changed according to building conditions such as the usage or location. When the indoor temperature is below 22 °C, heating operation of FCU starts in winter and when it is 24 °C, the operation stops. When the operation time and the room temperature meet the requirements for the heating operation, the heating operation using the heat storage tank is performed considering the temperature of the heat storage tank first. The heating using the heat storage tank is a method in which increases the utilization efficiency of the solar thermal energy in consideration of the case where the production time and the usage time of the solar thermal energy are different. If the temperature of the storage tank is low or if the heating operation using the storage tank is not performed, the heating using the solar thermal energy is performed.

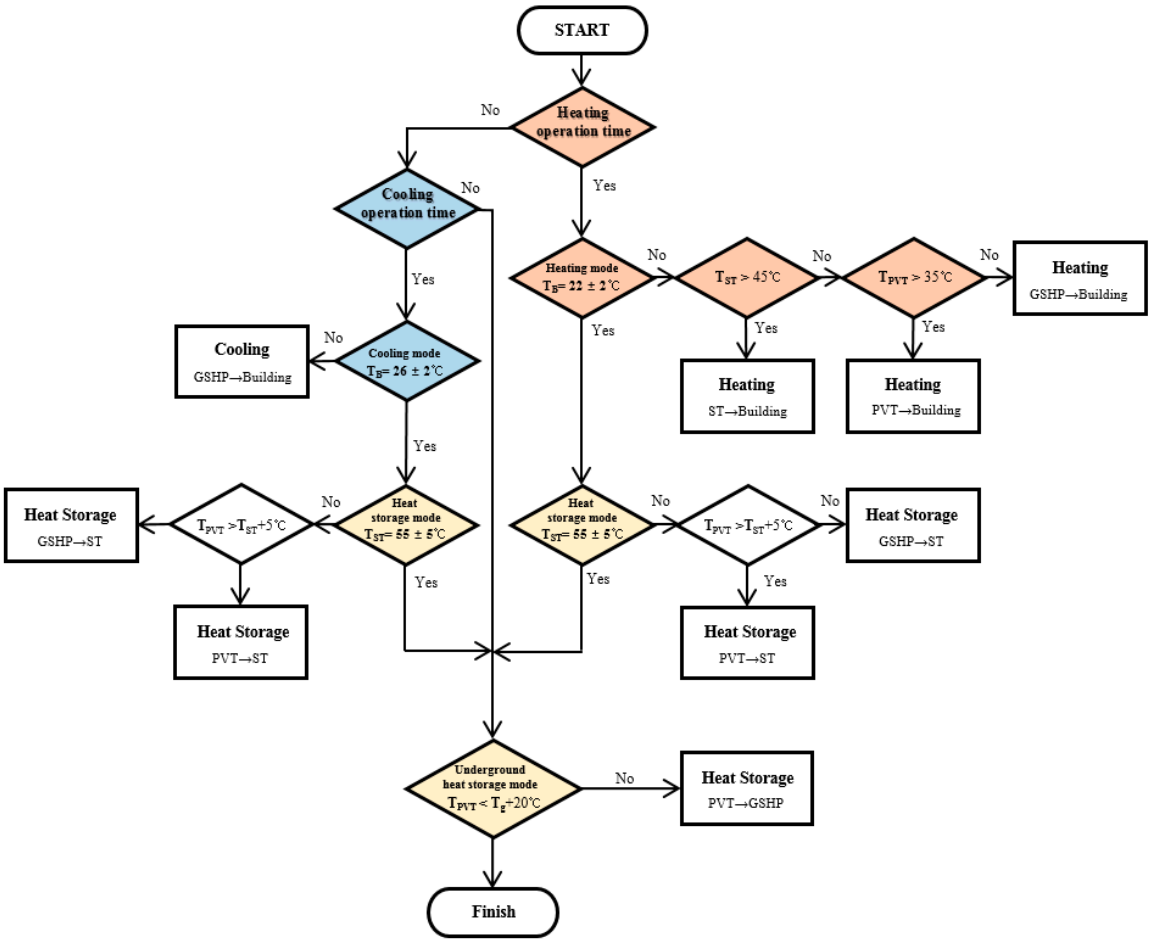

Figure 3. Control algorithm of Geo-PVT system in simulation.

Considering the heat source supply temperature of the heat pump and the temperature of the heat storage tank, the heating using solar heat is set to be supplied directly to the building when the temperature exceeds 35 °C. When the heating operation using the heat storage tank and the solar heat is not performed, the heating operation using the ground source heat pump is performed. The heat storage operation works when the temperature of the heat storage tank is reduced to 50 °C or less under the condition that the heating operation is not operated. The heat-storage operation mode can be divided into the following two types according to the type of heat source: use of the PVT module and use of the heat pump. When the outlet temperature of the PVT module is higher than the outlet temperature of the HST load-side, the heat-storage mode operates to use solar heat. The heat-storage mode using the heat pump works when the PVT module is not used. The underground heat storage

mode can be operated to prevent reduction of the electrical efficiency and to recover the underground temperature. This mode operates if the outlet temperature of the PVT module is higher than the underground temperature during non-heating or non-heat-storage operations.

2.3. Calculation Method for the System Performance

Figure 4 indicates the simulation modelling of Geo-PVT system implemented in TRNSYS in order to calculate the system performance. As shown in Figure 4, it is composed with a standard u-type ground heat exchanger (type557a), water to water heat pump (type927), (type 560), heat storage with variable inlets and uniform losses (type 64), 4 pipe performance fan coil for FCU (type987), pump (type3d), valve, and etc. In order to model the thermal behavior of a building model, a multi-zone building component (type 56) was utilized, which reads the building description from an external file generated based on user supplied information with program called TRNBuild. The geometric model of the building was established through the TRNSYS 3D plugin for Google Sketchup, and export it to TRNBuild for TRNSYS simulation. Through the 3D model, all thermal zones to simulate in TRNSYS have been drawn.

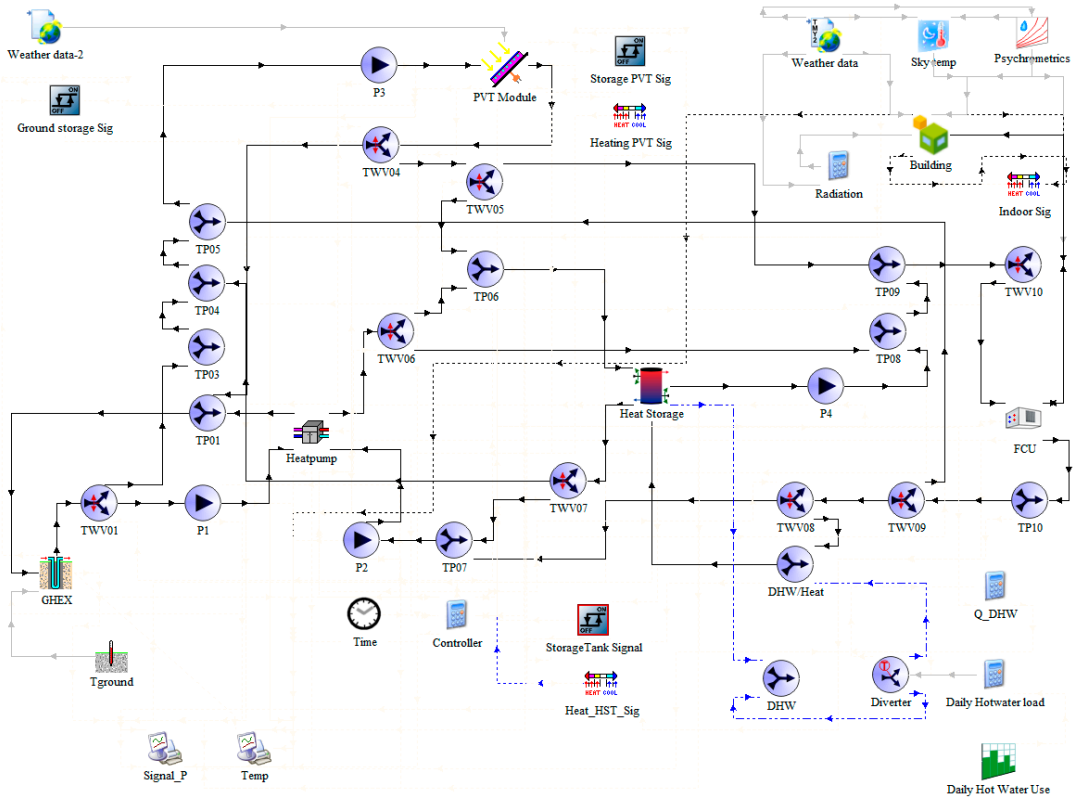

Figure 4. Simulation modelling of Geo-PVT system.

The simulation determines whether the heat source system corresponds to heating and hot water load of the building model and its performance. Here, corresponding to the hot water load is determined so as to judge whether the thermal energy supplied from the heat storage tank satisfies the hot water load. The calculator component was utilized to describe that the amount of hot water load is supplied from the heat storage tank every day, which is calculated by the daily hot water supply amount of the building. The hot water is to be supplied at 45 °C from the storage tank as much as the amount of hourly hot water demand, and the storage tank is filled back to maintain the tank level with water at 15 °C as much as the used hot water. The water temperature 15 °C is set considering underground temperature because the storage tank is buried in ground.

A U-tube type GHE model was utilized as a component of the ground-heat duct storage (DST) model which is developed by Hellström in the mathematical-physics laboratory at Lund University in Sweden [16]. According to the DST model, the GHE-outlet temperature is calculated as follows:

$$T_{GHE,out} = \beta T_{GHE,in} + (1 - \beta) T_{ground} \quad (1)$$

Here, $T_{GHE,in}$ is the inlet temperature of ground heat exchanger. In this model, if the fluid flow rate approaches zero, the outlet temperature reaches the surrounding ground temperature T_{ground}.

β is a damping factor that is defined as follows:

$$\beta = exp\left(-\frac{\alpha_v V}{C_f Q_f}\right) = exp\left(-\frac{\alpha_p L_p}{C_f Q_f}\right) \quad (2)$$

The thermal model of the PVT component relies on the algorithms presented in the "flat plate collectors" section of the Solar Engineering of Thermal Processes textbook by Duffie and Beckman [17]. The mean absorber-place temperature can be used to calculate the energy rate Q_u at which is added to the flow stream by the collector, as follows:

$$Q_u = A_c[S - U_L(T_{abs} - T_{amb})] \quad (3)$$

where A_C is area of the solar collector. This can be either gross area or net area but should be consistent with the provided loss coefficients and PV power conversion coefficients. The overall loss coefficient of the collector U_L is the sum of the top (U_t), bottom (U_b), and edge (U_e) loss coefficients.

The power generation of the PVT module can be estimated by multiplying the solar energy incident on the surface with the efficiency of the photovoltaic module, as following Equation (4). S is the net absorbed solar radiation and accounts for the absorbed solar radiation minus the PV-power production. Equation (5) is the formula to calculate S. The efficiency of the PV cells is a function of the PV cell temperature and the incident solar radiation, as following Equation (6). Figure 5 indicates the efficiency of the PV cells as a function of the cell temperature at the constant radiation:

$$Power = (\tau\alpha)_n (IAM) G_T (\eta_{PV}) \quad (4)$$

$$S = (\tau\alpha)_n IAM G_T (1 - \eta_{PV}) \quad (5)$$

$$\eta_{PV} = \eta_{nominal} X_{CellTemp} X_{Radiaion} \quad (6)$$

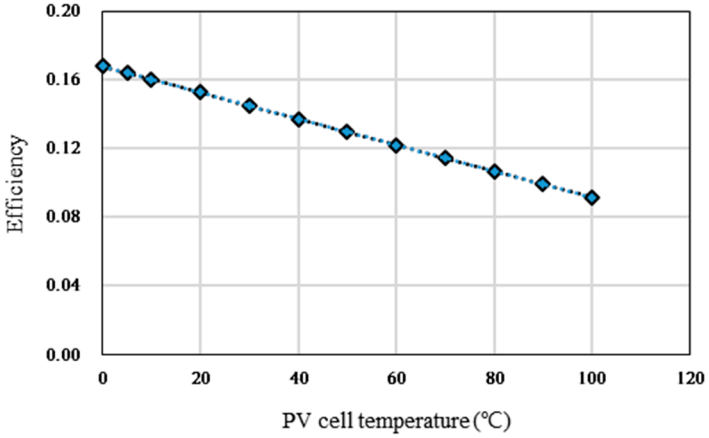

Figure 5. Efficiency of PV cell as a function of the cell temperature at a 350 W/m^2 radiation.

Under off-normal conditions, the transmittance-absorptance product at normal incidence is multiplied by the following equation in order to get the transmittance-absorptance at other incidence angles. This equation is referred to as the incidence angle modifier (*IAM*):

$$IAM = \frac{(\tau\alpha)}{(\tau\alpha)_n} = \frac{G_{bT}\frac{(\tau\alpha)_b}{(\tau\alpha)_n} + G_{bT}\frac{(1+cos\beta)}{2}\frac{(\tau\alpha)_s}{(\tau\alpha)_n} + G_{bT}\rho_g\frac{(\tau\alpha)_g}{(\tau\alpha)_n}}{G_T} \quad (7)$$

The heat pump performance is based on the entering source-side and load-side temperatures and is in accordance with the catalog data. The heat-pump catalog data is shown in Figures 6 and 7. It was set that the ground-heat exchanger is a single U-pipe buried in a vertical borehole at a depth of 150 m. To explain more about other components, the heat storage model expresses the thermal performance of a fluid-filled sensible energy in storage tank. And the FCU model represents a fan coil where the air is heated or cooled as it passes across coils embracing hot and cold liquid flow streams. Plus, the pump model is simply set to a mass flow rate using a variable control function.

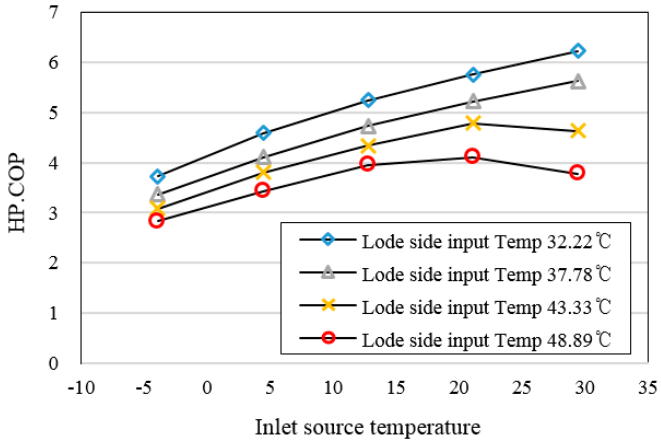

Figure 6. Heating catalog data of heat pump.

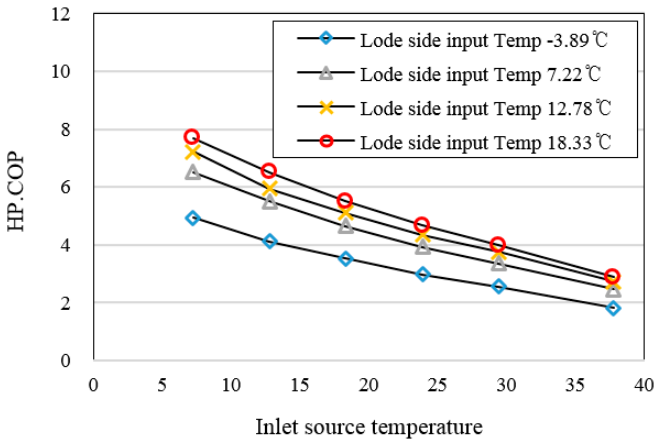

Figure 7. Cooling catalog data of heat pump.

System performance is calculated by the total energy consumption and total energy production. In this paper, the fixed time step in the simulation statement is 5 min, and the system performance was estimated by the seasonal performance factors (SPF_{HP}, SPF_{Solar}, and SPF_{System}) based on the simulation results in each case. Here, the seasonal performance factor is a coefficient that can be obtained by dividing the total cooling and heating energy during the heating and cooling season by the total power consumption. The calculation formula is as following Equations (8)–(10). The calculation process

is illustrated in Figure 8. "Q" represents the useful energy from the output of the system, and "P" represents the sum of all of the input electrical energy that is required to produce the useful energy. This method is based on the report of IEA Task 44 Annex 38:

$$\boldsymbol{SPF_{HP}} = \frac{Useful\ energy(Heat\ pump)}{Input\ energy(Heat\ pump)} = \frac{\int (Q_{HP\to B} + Q_{HP\to ST})\ dt}{\int P_{HP}\ dt} \tag{8}$$

$$\boldsymbol{SPF_{Sol}} = \frac{Useful\ thermal\ energy(PVT)}{Input\ energy(PVT)} = \frac{\int (Q_{PVT\to G} + Q_{PVT\to ST} + Q_{PVT\to B})\ dt}{\int (P_{P3,G} + P_{P3,ST} + P_{P3,B})\ dt} \tag{9}$$

$$\begin{aligned} \boldsymbol{SPF_{Total\ system}} &= \frac{Useful\ energy(System)}{Input\ energy(System) - produced\ energy(PVT)} \\ &= \frac{\int (Q_{PVT\to B} + Q_{HP\to B} + Q_{ST\to B} + Q_{DHW})\ dt}{\int (P_{system}\ dt - \int P_{PVT,Production})\ dt} \end{aligned} \tag{10}$$

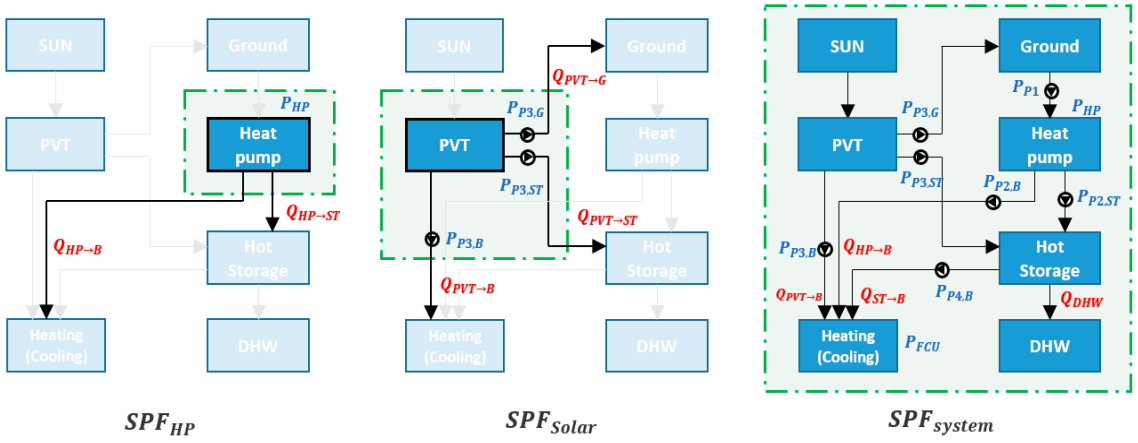

Figure 8. Calculation method of SPF.

2.4. Economic Evaluation Model of Geo-Photovoltaic/Thermal System

In this study, the feasibility of the proposed hybrid system was evaluated based on a return on investment (ROI) analysis including initial cost, operating cost and maintenance cost of the Geo-PVT system compared with the GSHP system.

The system capacities were designed for peak load of building model. The capacity of ground source heat pump system was settled considering peak load and safety rate. A PVT module (1.63 m^2) was assumed to have heat capacity of 0.3 kW based on simulation result. For this reason, it was assumed that 20 m^2 of PVT system has as same capacity as 1RT (3.5 kW) of GSHP system.

In this paper, the Geo-PVT system was made up with the PVT system, which replaced 1RT (3.5 kW) of heat pump capacity. During heating operation, hybrid system is available to reduce the capacity of heat pump. However, the heat pump capacity should not be lower than cooling peak load because only heat pump system can respond to cooling load.

The system power consumption was calculated through the simulation considering the ground temperature. As for ROI analysis, life cycle cost (*LCC*) was calculated for 20 years, and it was analyzed in two cases; one case is that the generated electricity of the PVT module utilized for operation, and the other case is that it is sold at the price of the power exchange. *LCC* analysis applied the net present value method and the calculation procedure is to add the recurring costs (P_A) and non-recurring costs (P_F), as following Equation (11) [18]. The inflation rate was set as 3.4%, which reflects the recent economic situation in Korea for a detailed prediction:

$$LCC = \frac{P_F}{i(1+i)^n} + \frac{P_A[(1+i)-1]}{i(1+i)^n} \tag{11}$$

In order to determine initial investment cost, the initial cost of each system was determined by referring to the renewable energy sources standard price and Korea On-Line E-Procurement System in Public Procurement Service [19,20]. Also, in order to estimate the maintenance costs, it was assumed that the life span of heat pump and PVT module were 20 years, and heat storage tank and circulating pump were replaced for every 10–15 years, respectively. The electricity unit price was followed by the standard unit price of Korean Electric Power Corporation (KEPCO) and the selling price of the electricity was referred to the System Marginal Price (SMP) from the Korea Power Exchange. The price from the SMP was set as 100.6 won/kWh, at average price.

2.5. Case Study

The building model for simulation was set as 106 m^2 standard housing supplied by the Ministry of Agriculture, Food and Rural Affairs in Korea, which is an authorized model with "representative" to be widely popularized. Therefore, the reliable model can provide a great ripple effect of the hybrid system. The building model is divided into two floors and accommodates a living room, four bedrooms, and a kitchen. The floor plan of the building is shown in Figure 9 [21]. The weather data of the simulation model is based on Seoul, South Korea, which was provided by Meteonorm. An average outside temperature and solar radiation in Seoul described in Figure 10.

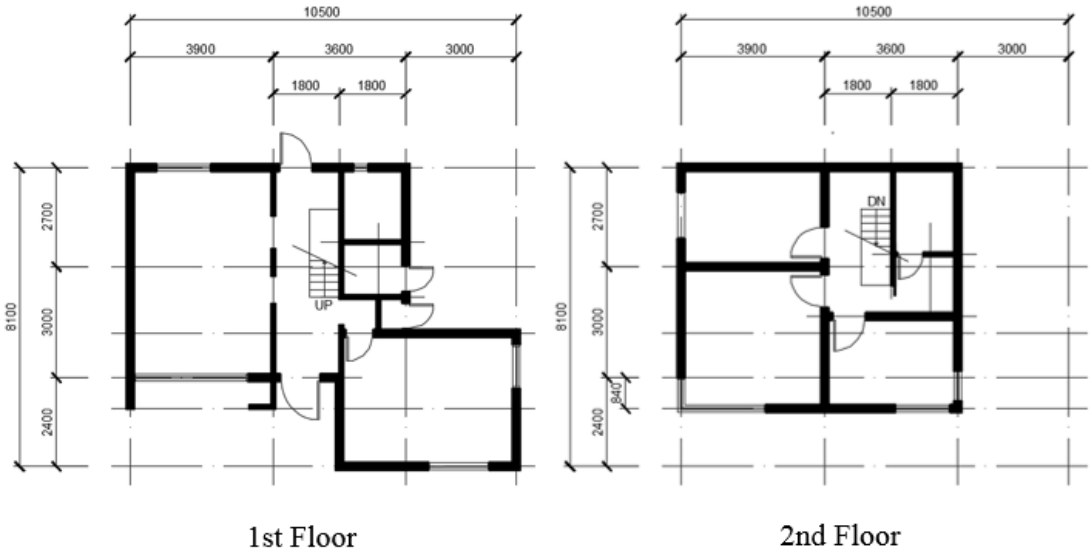

Figure 9. The building model for simulation.

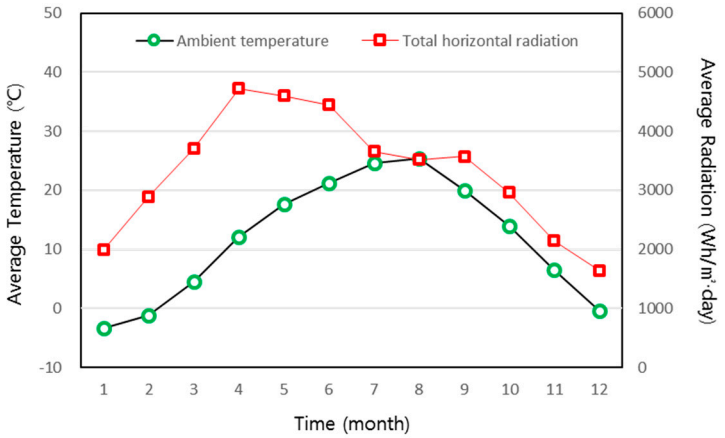

Figure 10. Weather data in Seoul.

Thermal properties for heating and cooling load analysis were set using the central-district standard of the "Korean Energy Saving Design Standards of Buildings" published by the Ministry of Land, Infrastructure and Transport [22]. The heating and cooling operation condition was referred from the handbook of the Society of Air-conditioning and Refrigerating Engineers of Korea, as outlined below [23]. The simulation-design parameters for the system-capacity calculation are shown in Table 1.

Table 1. Basic simulation design parameter.

Contents		Value	Units
Location		**Seoul, Korea**	
Simulation time		November–October	Month
Simulation time step		5	Minutes
Design temperature		Heating 22, Cooling 26	°C
Operation Time		08:00~20:00/20:00~08:00	Hour
Ventilation		1/h	
Building model		Affordable Housing Model 'N-14-27'	
Total floor area		106	m^2
Heat transmittance	Roof	0.269	0.269 W/m^2 K
	Floor	0.405	0.405 W/m^2 K
	External wall	0.269	0.269 W/m^2 K
	Windows	2.1	2.1 W/m^2 K

The heating load of the building was calculated to determine the capacity of the system. The peak heating load was verified as 8.34 kW for the heating period in the target area. By using the peak heating load as the basis, the GSHP capacity was configured. The peak heating and peak cooling loads for Seoul are shown in Figures 11 and 12. The capacity of the heat pump, for which the peak heating load is considered, was determined as 10 kW.

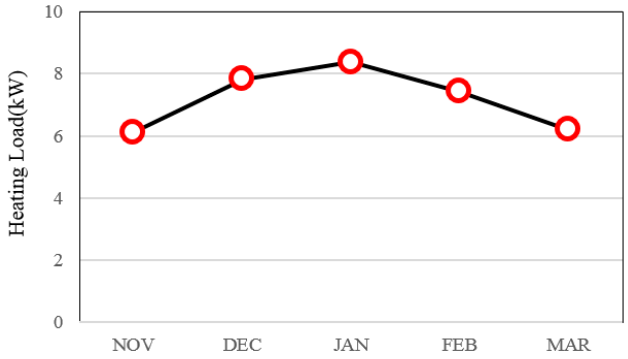

Figure 11. The peak load of heating season.

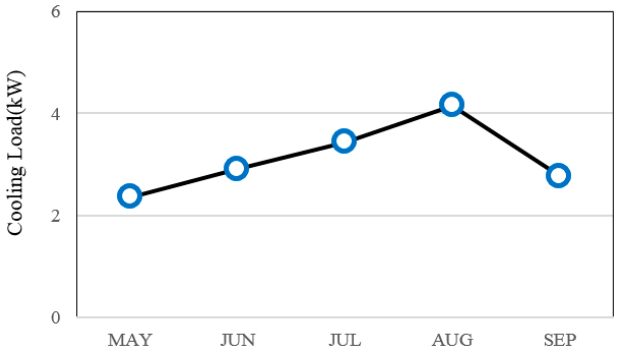

Figure 12. The peak load of cooling season.

The thermal properties of the soil was based on the features of granite which is widely distributed in Korea. The capacity of the PVT system was determined as 3 kW in consideration of the power consumption of the heat pump, which was the maximum capacity for a residential house that can receive a subsidy from the Korea Energy Agency. The PVT module with a 15.33% electrical efficiency was used referring to the preceding research study [24]. The solar absorption area of the PVT system in one module was 1.63 m^2, so the total area is 20 m^2. The detailed conditions were set according to those in Table 2. The daily flow-rate distribution of domestic hot water (DHW) is described in Figure 13, and the daily DHW distribution profile was based on the advanced research [25].

In this paper, the performance of the Geo-PVT system was analyzed and it was compared with a conventional GSHP system. Furthermore, the Geo-PVT system having HST was compared with the Geo-PVT system without HST and the system performance according to the set-point of PVT usage was calculated. Moreover, a simulation was conducted to find effective usage of the produced heat from PVT. In addition, an economic evaluation regarding cost-saving that is related to the installation of the proposed hybrid system was performed. Here, the heating capacity of the GSHP was replaced by the solar heating of the PVT system. To develop the Geo-PVT system, a feasibility study was assessed according to the initial and operating costs of the Geo-PVT system, and a comparison analysis was performed. An optimal design depending on the building-floor areas was suggested by a return-on-investment analysis.

Table 2. The parameters of Geo-PVT system in rated condition.

Component	Description	Value
Heat pump	Capacity	10 kW (water to water type)
	Flow rate	0.42 kg/s (Load side) 0.5 kg/s (Source side)
Ground heat exchanger	Type	Closed type single U-tube
	Borehole depth	150 m
	Number of boreholes	1
	Borehole radius	0.1 m
PVT Module	Module Type	Unglazed water type
	Collector width x length (Area)	4.92 m × 3.96 m (19.5 m^2)
	PV efficiency	15.33%
	Orientation/Slope	South/45°
Heat storage tank	Tank volume	0.3 m^3
	Heat loss coefficient	0.694 W/m^2 K
Fan coil unit	Rated total cooling/heating capacity	12 kW
	Rated volumetric air flow rate	0.3 m^3/s
	Power consumption	0.15 kW
Circulation Pump1 (Heat pump source side)	Flow rate	0.5 kg/s
	Power consumption	0.25 kW
Circulation Pump2 (Heat pump load side)	Flow rate	0.42 kg/s
	Power consumption	0.22 kW
Circulation Pump3 (PVT module circulation)	Flow rate	0.42 kg/s
	Power consumption	0.22 kW
Circulation Pump4 (ST—FCU circulation)	Flow rate	0.42 kg/s
	Power consumption	0.25 kW
Soil Conditions	Storage thermal conductivity	3.5 W/m^2 K
	Storage heat capacity	2520 kJ/m^3 K

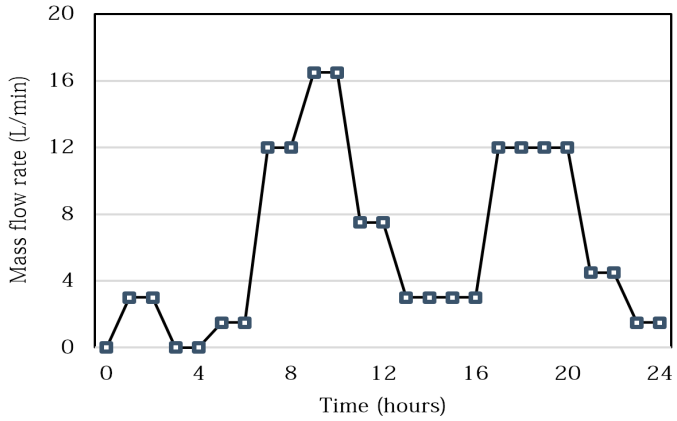

Figure 13. The supply pattern of daily DHW.

3. Validity of the Simulation Model

In this study, in order to verify the validity of simulation model, the simulation result was compared with the experimental result. The performance of the solar cell was measured according to the standard test condition (STC) specified in the IEC regulations, which are the solar radiation of 1000 W/m^2, the spectrum of AM 1.5 standard, and the solar cell temperature of 25 °C. In this experiment, the electrical performance according to the ambient temperature and the circulating water temperature was measured based on the test results under the standard test conditions. A fixed amount of irradiation intensity was maintained using a solar simulator and the electric current—voltage performance was measured according to the ambient temperature and the inlet temperature of the circulating water.

The constant temperature and humidity chamber used in the experiment was the AL SEC4100 manufactured by ATLAS (Linsengericht, Germany), and the artificial light source was irradiated using a metal halide lamp (Uniformity Class B) capable of adjusting the emission spectrum as the light source. The DS-100c I-V curved tracer was used to measure the electric current-voltage performance. The surface temperature of the module was measured using a thermocouple thermometer at the center of the top, middle, and bottom of the module, and data was recorded using a GL820 Data Logger (Graphtec, Yokohama, Japan). Table 3 indicates the specification of the measurement equipment. Experiments using a prototype PVT module were carried out at a solar photovoltaic center located at Techno Park (Chung-buk Province, South Korea). The nominal specifications of the PV module used in the experiment are listed in Table 4.

Table 3. Specification of the measurement equipment.

Equipment	Comments	Item
Solar simulator	Wave range 400~100 nm	-
	Measurement accuracy ± 2% ± 2 digit ± 0.4 digit/°C	
Temp & Humid Chamber	Temperature range −40 °C 150 °C Uniformity ±1 °C	ALSEC 4100
	Humidity range 20~98% RH Uniformity ± 3.0% RH	
Light source	Continues Type, Uniformity : Class B	Metal halide lamp
***I-V* test system**	1000 Volts; 3 ranges 1000 V, 100 V, 10 V/100 Amperes; 3 ranges 100 A, 10 A, 1 A	DS-100c I-V Curve tracer
Data logger	20 ch, Expandable up to 200 ch by unit of 20 ch	GL820 Data logger

Table 4. Photovoltaic module electrical characteristic.

Electrical Characteristics	Value	Units
STC Nominal maximum output power	250	W
Open circuit voltage	36.78	V
Short circuit current	8.93	A
Nominal maximum output voltage	30.46	V
Nominal maximum output current	8.21	A
Maximum system voltage (*V*)	1000	V
Module size	1644 × 992 × 40	mm
Module conversion efficiency	15.33	%
Cell type	Single crystal	-

In the experiment, an unglazed type of PVT-water module was used and the photovoltaic cells of the PVT module were single crystal photovoltaic cells with an electrical efficiency of 15.33% under standard temperature conditions. The PVT module combined an aluminum type of absorber plate and a circulating water pipe with copper to enhance heat transfer performance. The performance experiment was carried out under conditions of illumination of artificial light source and circulation of fluid in the PVT module.

Figure 14 is a scheme of the performance experiments. The temperature of the circulating water was set at 10 °C, 15 °C and 20 °C considering the system connection with GSHP system. The flow rate of the circulation water was set to 0.083 kg/s. Table 5 shows the experimental results compared with the simulation data in terms of surface temperature, thermal and electrical efficiency.

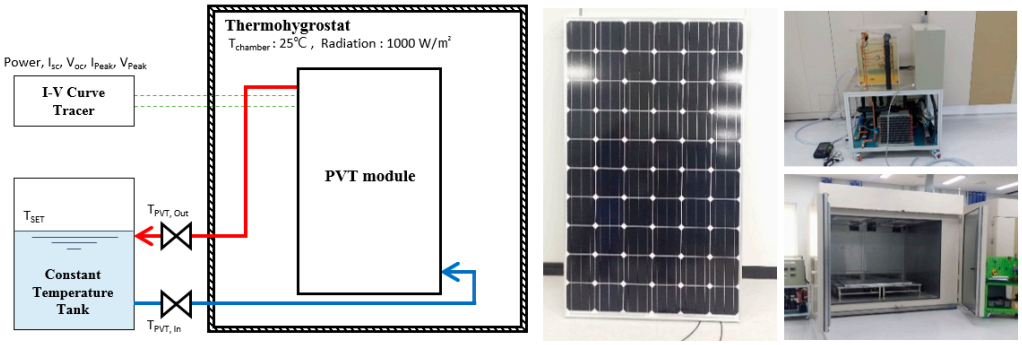

Figure 14. Scheme of the PVT performance experiment.

Table 5. Experiment results of the PVT performance experiment [24].

Section	Circulating Water Temperature 10 °C			Circulating Water Temperature 15 °C			Circulating Water Temperature 20 °C		
Contents	**Simulation**	**Test**	**Error Rate**	**Simulation**	**Test**	**Error Rate**	**Simulation**	**Test**	**Error Rate**
Surface Temperature	38.7 °C	39.5 °C	2.03%	42.5 °C	40.1 °C	5.99%	46.4 °C	41.0 °C	13.17%
Thermal Efficiency	65.28%	69.40%	5.94%	65.67%	65.50%	0.26%	60.00%	64.62%	7.15%
Electrical Efficiency	13.90%	13.20%	5.30%	13.60%	13.10%	3.82%	13.31%	13.10%	1.60%

As a result, thermal and efficiency decreased as the temperature of the circulating water increased. Generally, the electrical efficiency of PV decreased due to overheating of the PV panel. However, in a PVT system, the temperature of the PV panel can be decreased by water circulation in a pipe behind PV panel. The result of the PVT surface temperature showed a maximum margin of error of 13.17% between the simulation and experiment. The largest margins of error in the thermal and electrical efficiency were 7.15% and 5.30%, respectively. Comparing the experimental results with the simulation results, they show a similar pattern according to the circulating water temperature, but the numerical

values are different. Even though the surface temperature result under the condition of a circulation water temperature of 20 °C had an error in the experiment, the others had a slight error, and it is assumed that the spectral irradiance and spectrum values of the solar cell were different from those used for the simulation.

4. Simulation Results

4.1. Performance Comparison between Geo-Photovoltaic/Thermal and Ground Source Heat Pump

The performance of the Geo-PVT system was compared with the conventional GSHP system. Figure 15 shows the conceptual design of the GSHP system and Geo-PVT system. In the Geo-PVT system, the ground source is the main heat-source for the base load. On the other hand, the GSHP which consists of a GHE, a heat pump, and a HST operates for all the heat production in building. The individual system (ground-heat exchanger, heat pump, and circulation pumps) capacity and the operating conditions of the GSHP were set to be the same as those of the Geo-PVT system.

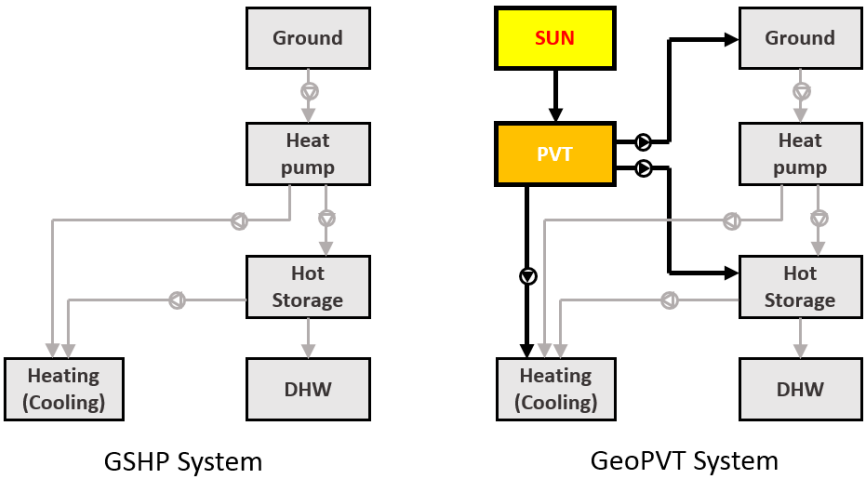

Figure 15. Conceptional design of GSHP system and Geo-PVT system.

The advantage of the hybrid system can be confirmed through the calculated system-performance factor. Prior to examining the monthly system performance during the heating and cooling period, the representative day was selected to examine the operation conditions based on quantitative figures with hourly thermal energy supply and energy consumption. The representative days chosen were 3 days when the heating load was the highest from 23 to 25 January, as shown in Figure 16.

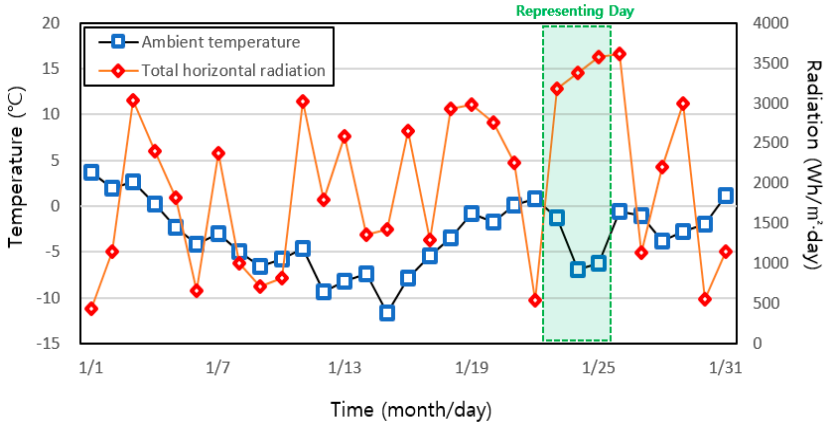

Figure 16. Ambient temperature and solar radiation in January.

Figures 17 and 18 show the hourly thermal energy supplied from the GSHP and Geo-PVT system of the representative day. The GSHP system supplied a total of 214 kWh of thermal energy to the building by operating the heat pump for 3 days. On the other hand, the Geo-PVT system supplied 192 kWh of thermal energy by working the heat pump, and produced 44 kWh of solar heat with the PVT system. The operation time of the heat pump could be reduced by using the solar heat source. The total heat pump operation time of the hybrid system for 3 days was 25 h and 30 min, which was about 12% lower than that of the GSHP system (28 h and 45 min).

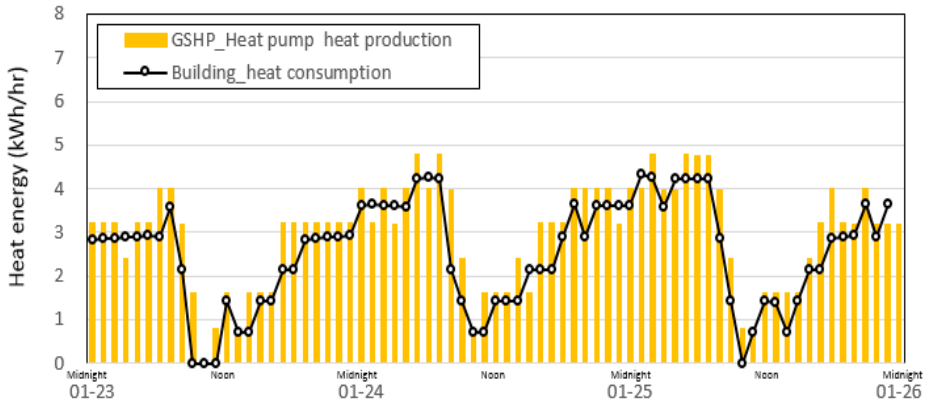

Figure 17. The heat production of the GSHP system during the representing 3-day period.

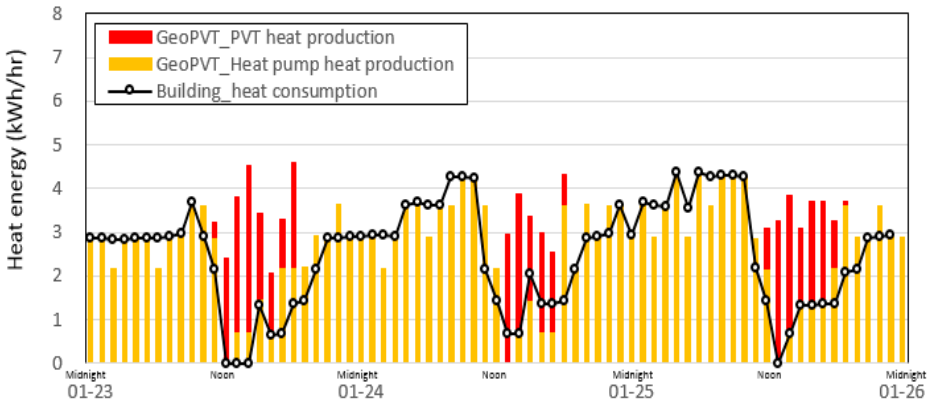

Figure 18. The heat production of the Geo-PVT system during the representing 3-day period.

Figures 19 and 20 show the power production and consumption of two systems on the representative days. The Geo-PVT system reduced the power consumption by about 6.5% compared to the existing system by reducing the operation time of the heat pump. The three-day power consumption of the GSHP system was 78 kWh and 73 kWh in the hybrid system. Plus, the hybrid system produced electric power of 35 kWh for 3 days through power generation of the PVT system.

The performance coefficient of the system was calculated by using the thermal energy production, power consumption and production. As a result of calculation of the coefficient of performance for three days during heating period, the GSHP system was confirmed to be 2.76, and the Geo-PVT system was confirmed to be 6.26. In this regard, it was confirmed that the operation time and the power consumption of the heat pump can be reduced through the use of the solar heat source. In addition, the performance coefficient of the system can be improved by using the production power of the photovoltaic module.

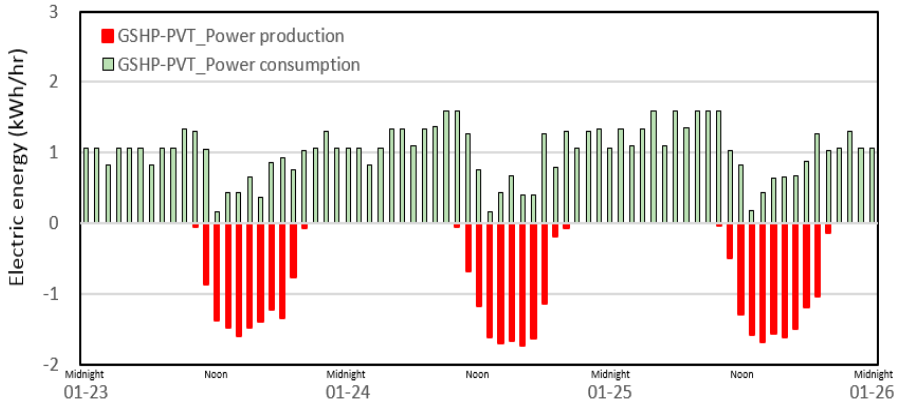

Figure 19. The electric energy of the Geo-PVT system in representing day.

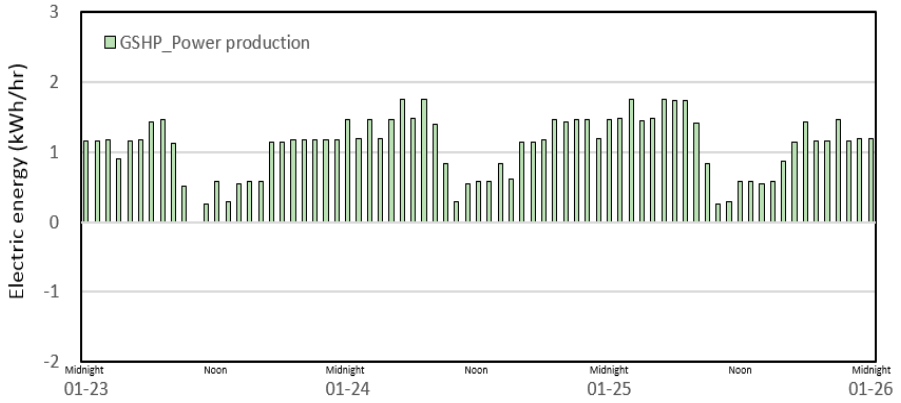

Figure 20. The electric energy of the GSHP system in representing day.

Figures 21–23 show the seasonal-performance factors of the GSHP and Geo-PVT system in each heating-operation time, respectively. During the entire calculation period, the performance of the Geo-PVT system was higher than that of the GSHP system. The SPF_{HP} of the Geo-PVT system increased by 4.6% for the daytime operation, 3.7% for the night-time operation, and 1.9% for the 24-h operation. It was figured out that the performance of the heat pump increased as the hybrid system utilized the solar heat source instead of the heat-storage mode decreased in the daytime operation. The SPF_{HP} values were 3.84 for the heating operation and 3.69 for the heat-storage operation, respectively.

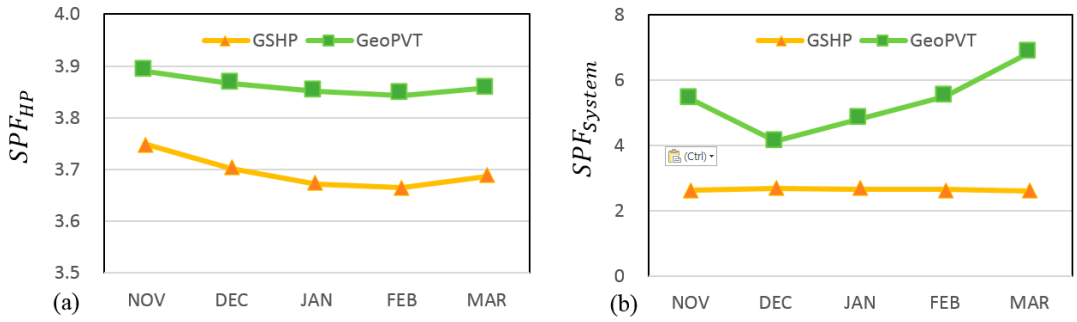

Figure 21. The result of SPF during daytime operation in heating season. (**a**) Heat pump; (**b**) system.

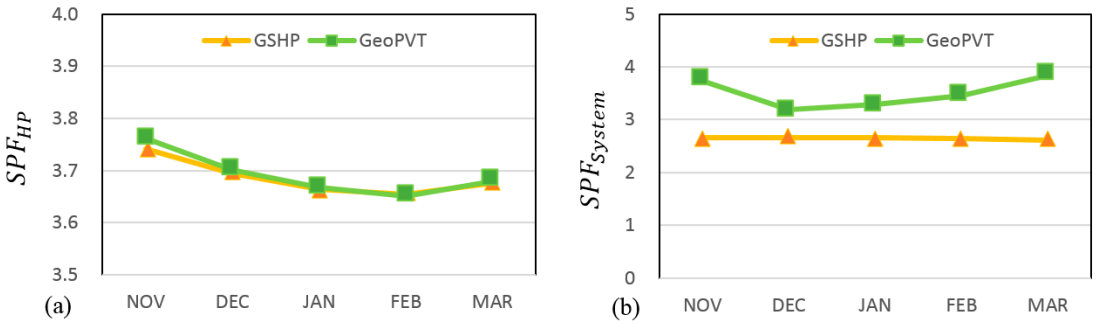

Figure 22. The result of SPF during night time operation in heating season. (**a**) Heat pump; (**b**) system.

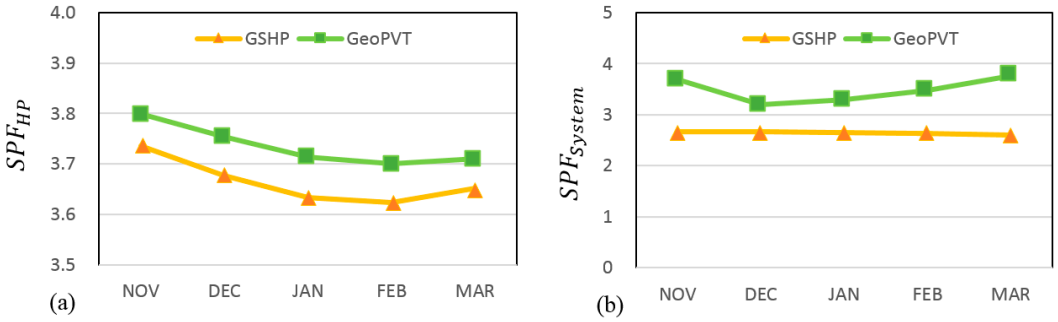

Figure 23. The result of SPF during 24 h operation in heating season. (**a**) Heat pump; (**b**) system.

For the daytime and 24-h operations, the solar heat was provided directly to the building load or heat storage. The amount of solar thermal energy produced was similar in both operation modes though the ratio of the supplied amount of solar thermal energy to total supplied thermal energy was about 17.18% during daytime operation and 6.05% in 24-h operation. For the efficient use of solar heat in the 24-h operation, the capacity of the PVT system needs to be larger due to the energy requirements of the building. During the night time operation, solar heat was used for the heat storage and the underground heat storage, and it was confirmed that the ratio of the produced thermal energy using solar heat to the total produced thermal energy was about 4.8%.

The SPF of the total system increased by the power production of the PVT module. The total SPF_{System} was 102% higher than that of the GSHP and the ratio of the electricity production to consumption was 38.27% during the daytime operation, which had low electricity consumption due to relatively high ambient temperature. The performance factor of the system was calculated as 3.50 for the night-time operation and 3.48 for the 24-h operation. The SPF of the hybrid system was 31% greater than that of the GSHP system. The ratio of the electricity production to consumption was 24.64% for the night-time operation and 20.45% for the 24-h operation, respectively, which were lower than those of the daytime operation.

Figures 24–26 represent the performance factors of GSHP and Geo-PVT systems from May to September, respectively. In cooling operation, the average SPF_{HP} was 3.82 in both the systems. The differences between the SPF_{HP} of the two systems were minor because of sole operation of heat pump for cooling operation. On the other hand, the SPF of total system in cooling season was observed to be high due to solar heat and electric power production of PVT system.

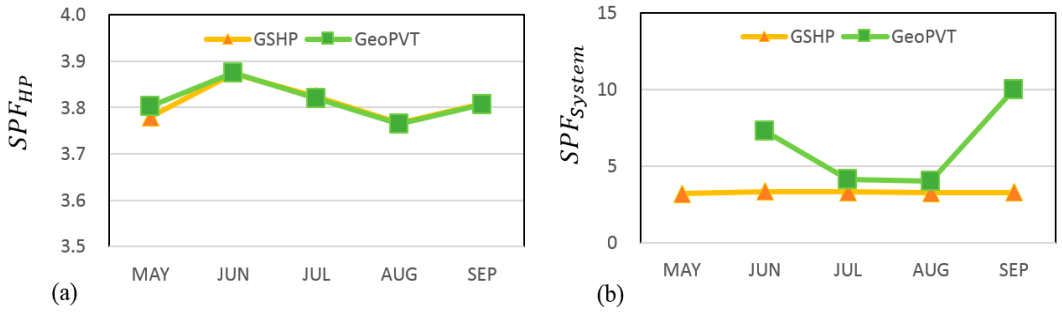

Figure 24. The result of SPF during daytime operation in cooling season. (**a**) Heat pump; (**b**) system.

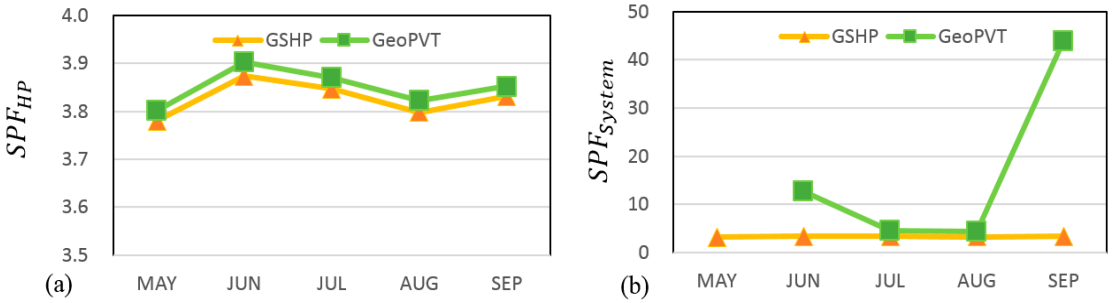

Figure 25. The result of SPF during night time operation in cooling season. (**a**) Heat pump; (**b**) system.

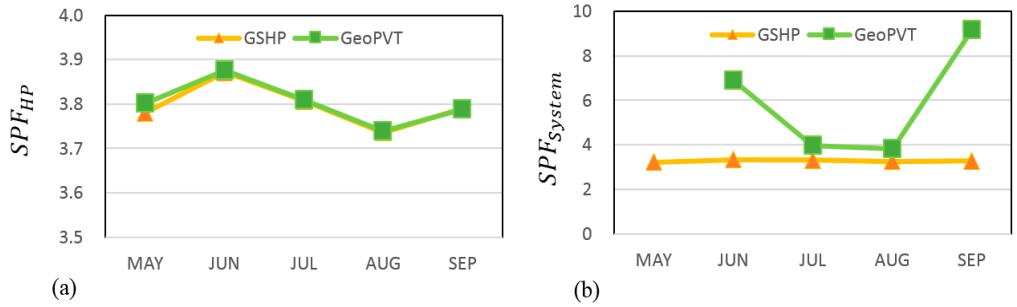

Figure 26. The result of SPF during 24 h operation in cooling season. (**a**) Heat pump; (**b**) system.

Power production of the PVT system in May surpassed the power consumption of the total system. The rise in performance factors was generally higher during May and September than other months. Based on the results of SPF_{System} in terms of operation times, the Geo-PVT system showed a 194% increase compared to GSHP system during day-time operation. Likewise, the SPF_{System} in night-time operation and 24 h operation were increased to 496% and 182%, respectively. The main reason of the significantly increased value for night-time operation was the reduced operation time of the heat pump compared with other operation modes.

4.2. Performance Analysis According to the Presence of Storage-Tank Heating

This section describes the system performance of the Geo-PVT system estimated according to the presence of HST. Figure 27 presents the system diagram of the comparison considering heating from HST. Although the operation with HST can be effective when the production time and supply time for solar energy do not coincide, the heat loss or additional installation cost of the HST should be considered. Considering the Geo-PVT system includes a HST, the storage tank should maintain a temperature above the hot-water-supply temperature. If heat is not gained from the solar energy, the GSHP system operates instead of the PVT system. However, as the load side temperature increases,

the performance of the heat pump decreases. Therefore, it is recommended to use direct geothermal heating without using a heat storage tank.

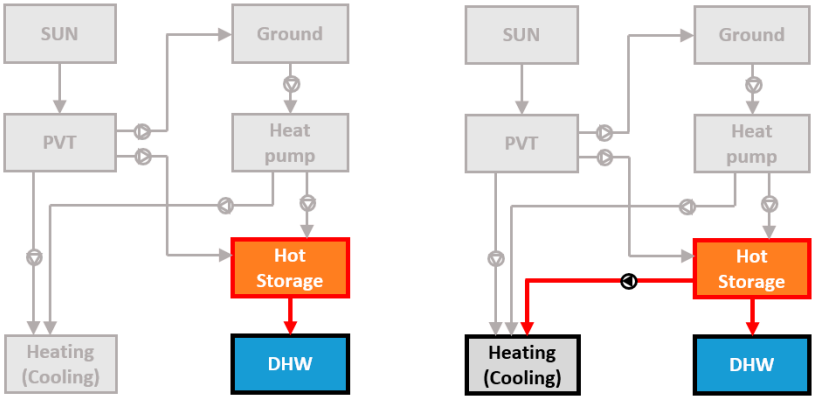

Figure 27. System diagram of comparison considering storage tank heating.

Figures 28–30 present the analysis results regarding the consideration of the tank-heating mode. When the HST is used for heating, the SPF of the heat pump is lower during the daytime operation and higher during the night-time and 24 h operations. It is judged that this was caused by the temperature difference on the load side of the heat pump flowing from the heat storage when the heat pump operates for heat-storage mode. Under the daytime-temperature condition, the heat-pump load-side temperature of the heat-storage mode was 43.71 °C, which was less than that of the heating mode. The heat-pump load-side temperatures was 51.63 °C for the night-time and 49.02 °C for the 24 h operation, respectively, which was higher than that of the heating mode. For the SPF under the daytime condition, the heat-storage operation increased more than the building-heating operation. In the case of the night-time and 24 h operations, the SPF increased by using the storage tank heating.

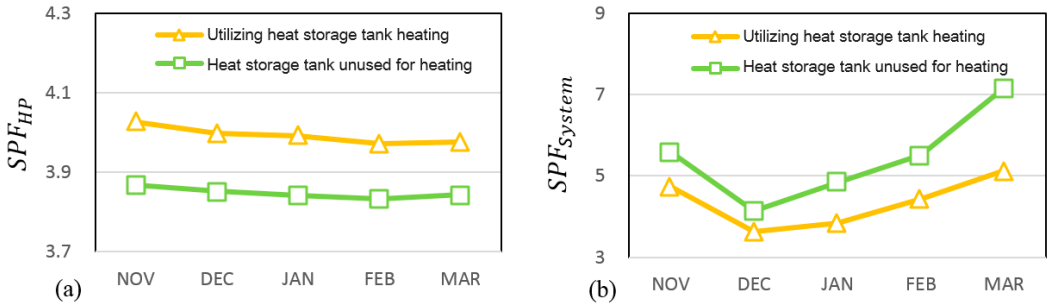

Figure 28. The SPF considering storage tank heating during daytime operation. (**a**) Heat pump; (**b**) total system.

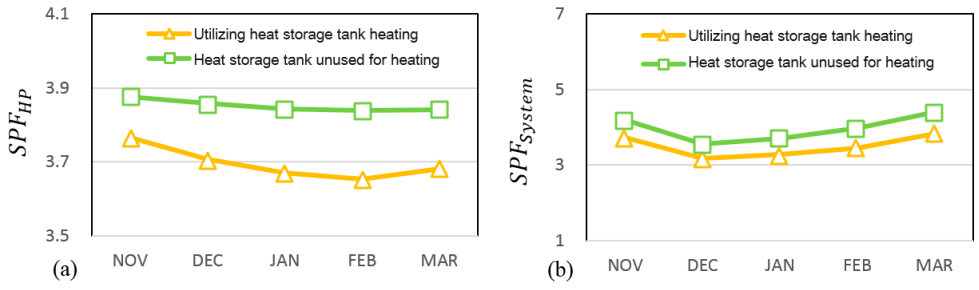

Figure 29. The SPF considering storage tank heating during night time operation. (**a**) Heat pump; (**b**) total system.

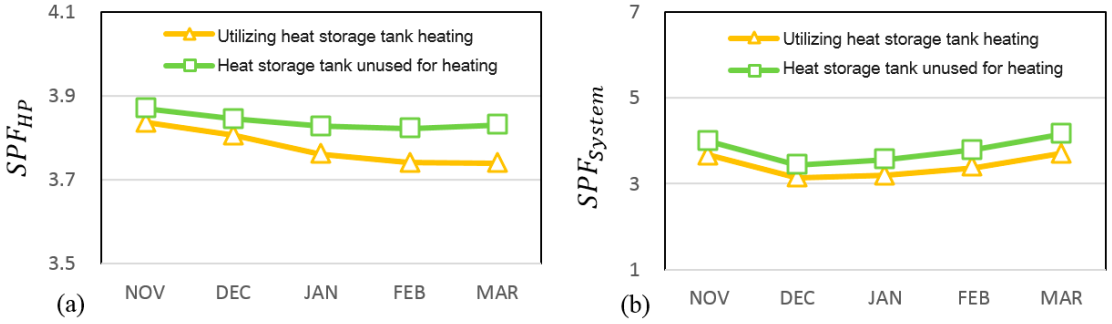

Figure 30. The SPF considering storage tank heating during 24 h operation. (**a**) Heat pump; (**b**) total system.

Under the daytime operation, the heating when the HST was used could achieve a heat production of 1050 kWh, which was 140% higher than that without using the HST. The 24 h operation increased by 18% and the night-time operation shows a small difference compared with the non-use of the storage tank for heating. The power consumption of the systemic operation that was calculated for the use of the circulation pump in the tank-heating mode increased due to the additional operation. This increase, which occurred under the daytime operation for the direct use of solar-heat production, was significant. When the system did not use the HST for building heating, the electricity consumption reduced by 3.76% for the daytime operation, 9.2% for the night-time operation, and 7.88% for the 24 h operation. These results suggested that when storage-tank heating was not used, the SPF of the total system increased for this operation condition. The SPF depends on the amount of the power consumption, and the rates of increase in the SPF were 24.96% for the daytime operation, 13.41% for the night-time operation, and 10.69% for the 24 h operation.

4.3. Performance Analysis According to the Set-Point Temperature of the Photovoltaic/Thermal

Figure 31 presents the heat production for the heating and heat-storage according to the set temperature using solar heat during the heating process is considered. The PVT-heat production is the lowest in December and the highest in January and February. It was found that the heat production of the PVT module was influenced by the heating load and the solar radiation. When the set temperature was 35 °C, the case achieved a heat production of 718 kWh for the heating during the simulation period, which was higher than those of the case with 40 °C (668 kWh) and the case with 45 °C (577 kWh) cases. The amount of heat stored in the heat storage tank reached 340 kWh and 342 kWh when the set temperature was 35 °C and 40 °C, respectively. As the set temperature increases, the heat production for heat storage decreased.

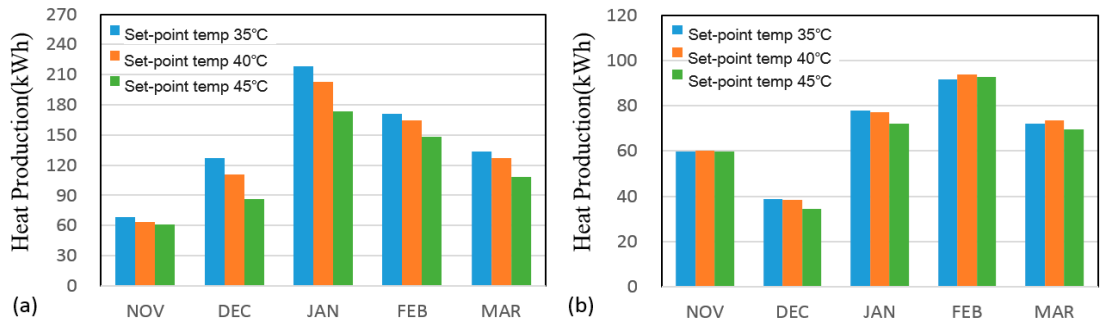

Figure 31. Heat production in PVT module (**a**) for building heating (**b**) for heat storage according to Change of solar heating temperature.

Figure 32a shows the SPF under the solar-heating condition. The SPF increased according to the set temperature of the PVT, and this is due to the increased temperature gap between the heat source and the building return air of the FCU. In the case of the set temperature 45 °C using solar heat, the calculated SPF was 22.79, which was 5.5% more than that of the case of 35 °C. Figure 32b shows the SPF for the heat-storage operation when the solar heat was used. The SPF of the heat-storage mode increased as the heating-supply temperature became higher.

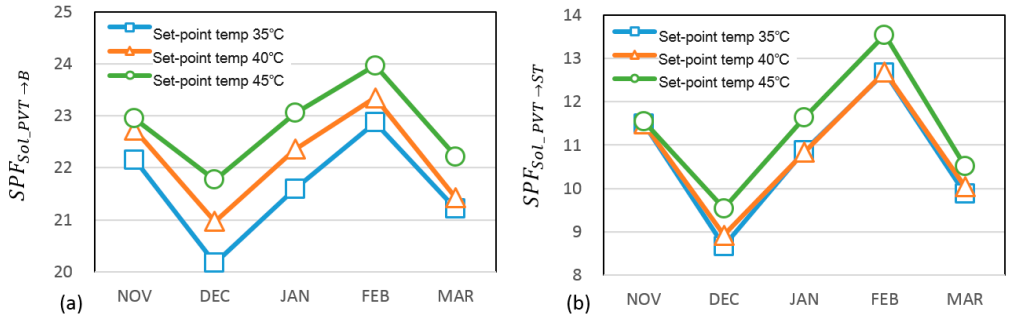

Figure 32. The SPF of PVT according to the set-point temperature of PVT. (**a**) For building heating; (**b**) for heat storage.

Figure 33a shows the SPF_{solar} according to the set temperature of the PVT. Regarding the SPF results for the heating mode and the heat-storage mode for which solar heat is used, the SPF increased according to the increasing of the inlet-water temperature. The SPF of the case 45 °C was 16.78, which was the highest result, and this increased by 2.3% more than that of the case 40 °C and by 2.7% more than that of the case 35 °C. Figure 33b represents the SPF_{System} according to the set temperature using solar heat. According to the calculated results, the SPF_{System} of the case 35° C was the highest as 3.45, and it decreased gradually according to the increasing of the set temperature. The SPF values for the 30 °C and 45 °C cases are 5.41 and 5.35, respectively. The difference between the conditions of the solar-heat temperature was 1.8%.

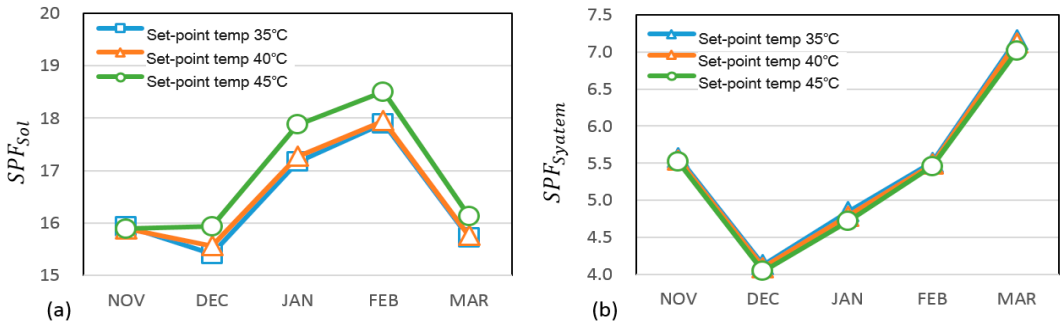

Figure 33. The SPF of total system according to the set-point temperature of PVT. (**a**) PVT; (**b**) total systems.

4.4. Performance Analysis According Operation Method of the Photovoltaic/Thermal

In this section, the system performance according to the usage of heat from PVT was analyzed. Figure 34 shows the conceptional design considering the operation method of heat from PVT module.

In operation (a), it provides heat from PVT to underground heat storage without heating and hot water. In operation (b), heat from PVT is not used in heating, but hot water. In addition, operation (c) provides the produced heat from PVT module to only space heating.

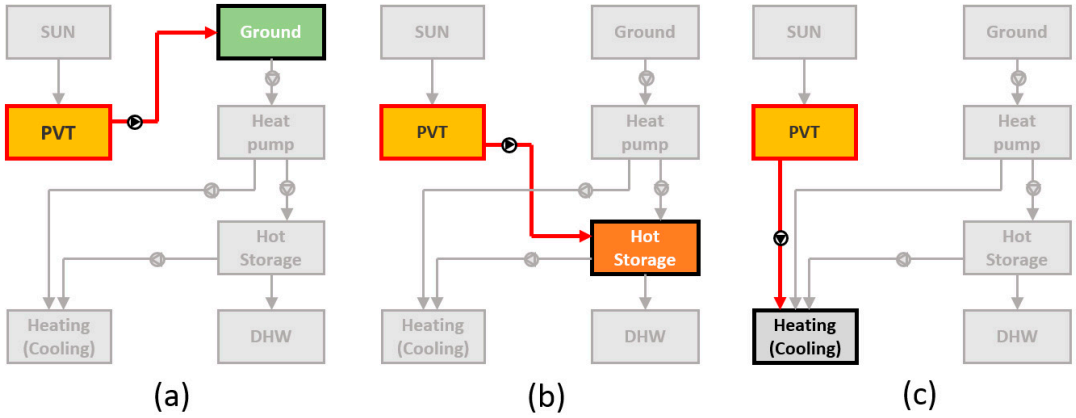

Figure 34. Conceptional designs considering connection method of PVT module. (**a**) Heat production to underground heat storage; (**b**) to hot water; (**c**) to space heating.

Figure 35a shows the heat production according to the connection method between the PVT and GSHP systems. The heat production was the highest in the underground heat storage at 949.29 kWh, and it was lowest in the heat storage at 437.50 kWh. In the solar-heating case, the heat production depended on the change of the heating load. The underground heat storage was influenced by solar radiation.

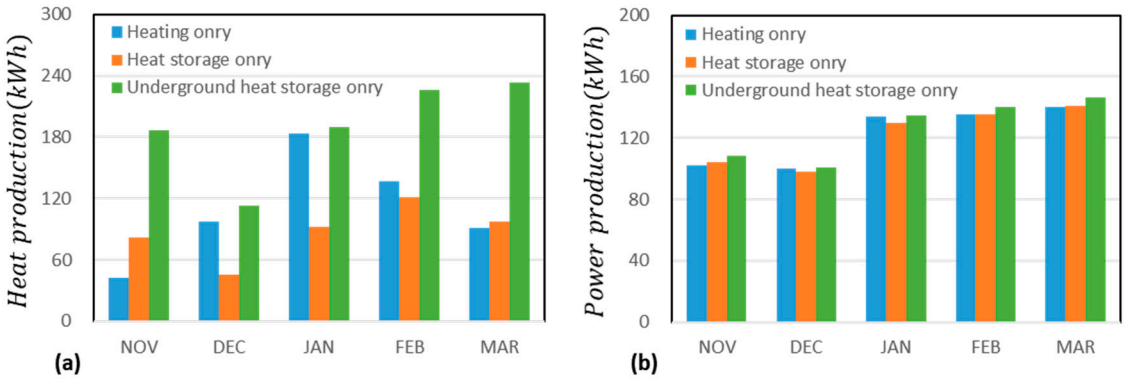

Figure 35. (**a**) Heat production; (**b**) electricity production of PVT system.

The electricity production is shown in Figure 35b. The electric power production was large in the condition of high heat production, and it was 629.93 kWh in the underground heat storage operation and 608.10 kWh in the heat storage tank heat storage operation. The figure shows the SPF of the PVT module according to the variety of solar-heat-usage methods. The SPF_{Solar} values of the method when using solar heat were 21.41, 11.33, and 19.32 when only heating, heat storage, and underground heat storage, respectively. Figure 36 shows the SPF_{System} according to the method of using solar heat. The SPF_{System} of the solar-heating case was 5.35 higher than those of the other cases because solar energy was used as the direct energy and the supply temperatures, which were calculated as 4.42 in the heat-storage case and 4.58 in the underground heat-storage case.

Compared with that for the solar-heating operation, the performance for the heat-storage operation decreased by 17.6%, and that for the underground heat-storage operation decreased by 6.0%. The heat production of the heat storage for the solar-heat condition was the lowest because the supply was the highest. The SPF value was low because the temperature difference between the heat source and the building temperature was reduced. In the case of underground heat storage operation, high heat production and efficiency were shown due to the supply temperature that can utilize the solar thermal energy efficiently. However, because of the characteristics of the operation of the underground

heat storage, the stored thermal energy was scattered to the ground, so that the ratio of the utilization was low. As a result, the performance of the PVT module was high but it did not affect the efficiency of the total system. In order to use this mode efficiently, a method of storing the stored heat was required to the operation of the heat pump.

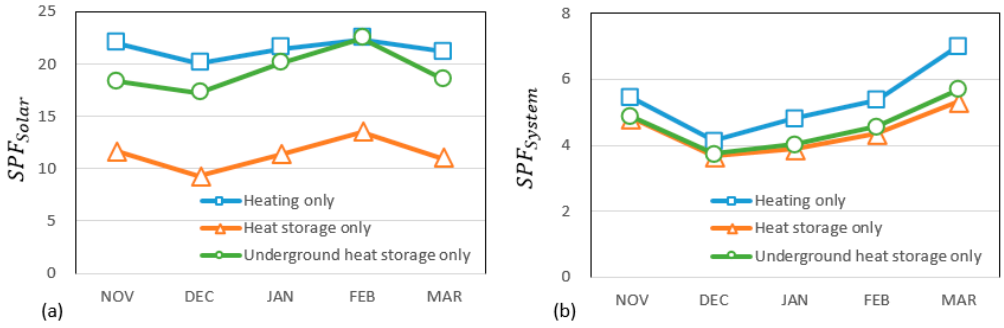

Figure 36. The result of SPF considering change method of using solar heat. (**a**) PVT; (**b**) total systems.

4.5. Economic Evaluation of Geo-Photovoltaic/Thermal System

In this study, in order to develop Geo-PVT system, feasibility study was evaluated, and the result was compared with the GSHP system. In addition, the present work illustrates optimal design by return on investment (ROI) analysis according to floor areas of building model, which were 99 m^2, 165 m^2, and 231 m^2. The capacity of ground source heat pump system was calculated as 10 kW for 99 m^2, 13.5 kW for 165 m^2 and 17 kW for 231 m^2 building areas, respectively. Figure 37 represents the initial costs of Geo-PVT system and GSHP system.

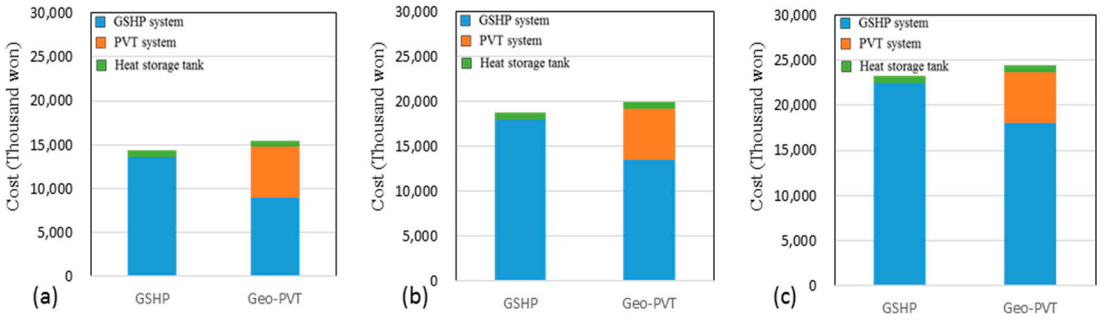

Figure 37. Heat production of PVT system considering change method of using solar heat. (**a**) 99 m^2 building area; (**b**) 165 m^2 building area; (**c**) 231 m^2 building area.

As the building area increases, the design capacity of the GSHP system was set as 3RT (10.5 kW), 4RT (14 kW) and 5RT (17.5 kW) based on the heating and cooling loads of the housing model. In Geo-PVT systems for each total capacity, the GSHP systems were designed as 7 kW, 10 kW and 13.5 kW including a 20 m^2 PVT system. Figures 38–40 show the power consumption and production through building heating and cooling operations in Seoul.

Figure 41 presents the result of LCC analysis when extra electric power was resold to the Korea Electric Power Corporation. Since the selling prices were higher than the electrical price, selling electric power was more economical than using the produced electricity. Compared with GSHP system, the payback period of Geo-PVT system was 7 years in the case of building area as 99 m^2, 10 years in the case of building area as 165 m^2 and 11 years in the case of building area as 231 m^2 building areas, respectively.

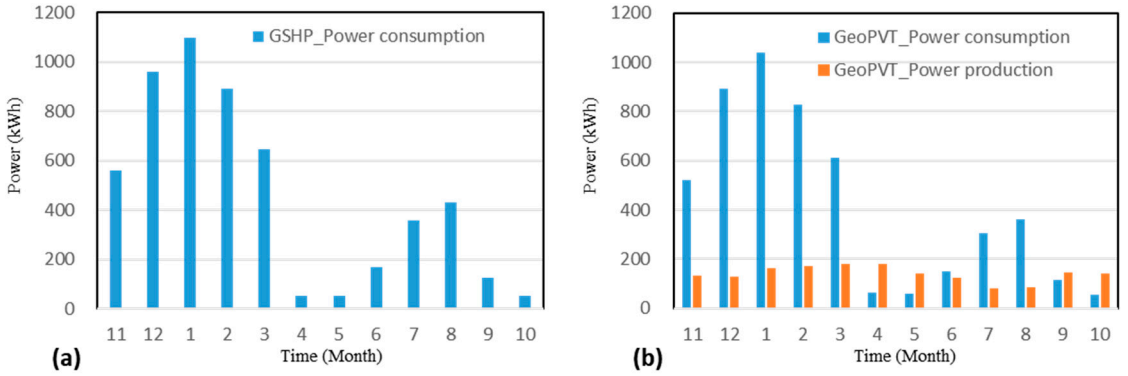

Figure 38. Power consumption and production of system in 99 m^2. (**a**) GSHP; (**b**) Geo-PVT.

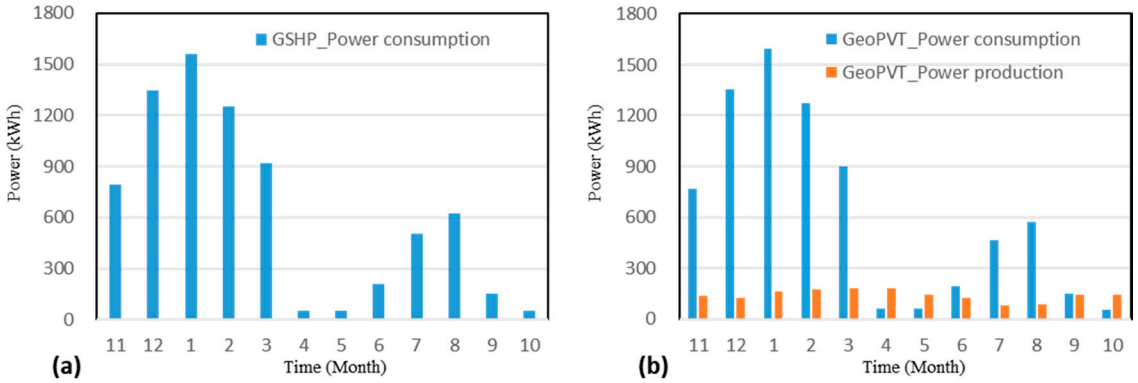

Figure 39. Power consumption and production of system in 165 m^2. (**a**) GSHP; (**b**) Geo-PVT.

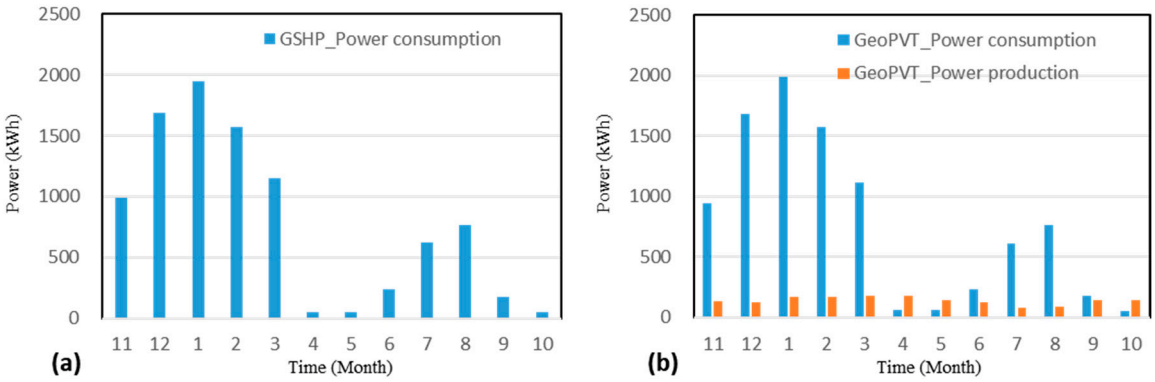

Figure 40. Power consumption and production of system in 231 m^2. (**a**) GSHP; (**b**) Geo-PVT.

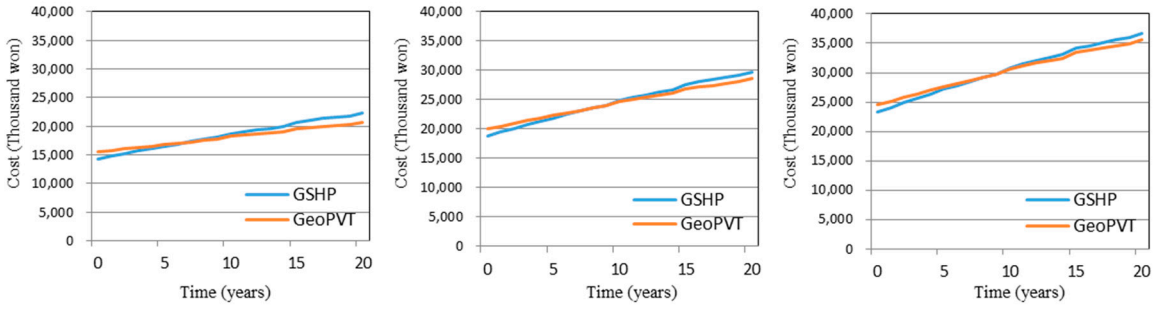

Figure 41. The result of life cycle cost.

5. Conclusions

In this paper, a performance prediction model of a hybrid system combining a photovoltaic-thermal system and a ground source heat pump system was established for the purpose of developing a renewable energy convergence system that produces reliable energy for building energy independence. A residential building in Seoul, Korea was modeled, and a performance analysis was performed using the simulation. Based on the results, a comparative analysis with the existing system was conducted. In order to improve the performance of the system, a case study was conducted. In the feasibility analysis of the introduction, the life cycle analysis of the system was performed considering the size of the building area. The results of this study can be summarized as follows:

- A PVT module (1.63 m^2) was assumed to have a heat capacity of 0.3 kW, so that 20 m^2 of PVT system has the same capacity as 1RT (3.5 kW) of GSHP system. In this paper, a 106 m^2 housing model located in Seoul, Korea was studied and the building system consists of a 10 kW GSHP (74% of the peak load), a 3.5 kW PVT system (26% of the peak load) and a 0.3 ton heat storage tank.
- The control logic was constructed by using the two heat sources and heat storage tanks of the hybrid system, and annual power consumption and heat quantity were analyzed through simulation analysis. As a result of 3 days of simulation, the PVT part of the hybrid system produced about 19% of total heat energy supply, reduced energy production using the GSHP system, and decreased operating time by 12%.
- According to the performance analysis of the hybrid system, it was confirmed that the SPF_{system} was increased due to the power production of the solar photovoltaic system. The average SPF_{system} during the heating period was 5.33 and increased by 102% compared with the existing system during the daytime of the building.
- The results of the performance analysis of the hybrid system according to the presence of the heat storage tank showed that SPF_{system} increased when the heat storage tank was used in the daytime operation, and when it did not operate in nighttime and 24 h.
- The SPF_{PVT} according to the set supply temperature was the highest at 5.45 at 35 °C, which was the lowest temperature of the heating set point, and the performance decreased as the set temperature increased. The SPF_{system} at 40 °C and 45 °C were 5.41 and 5.35, respectively, and the performance difference according to the supply temperature was found to be 1.8%.
- Considering usage method of the solar heat source, the SPF_{system} was the highest at 5.35 in the heating operation using solar heat. It was 4.42 under the condition that the solar heat was used for the heat storage and 4.58 in the case of the heat storage in the ground.
- As a result of the feasibility assessment, it was confirmed that the initial investment cost of the hybrid system was higher than that of the existing GSHP system, but the annual operating cost was reduced and the investment cost could be recovered after about 7~11 years.

The performance of the hybrid system has been verified through dynamic and transient performance analysis using the energy simulation, and the best performance was demonstrated according to the heat storage tank, the supply temperature and the operation method. This study provides a quantitative analysis of a hybrid system for a specific area and building type. In the future, an optimal sizing for the Geo-PVT system will be analyzed considering building scale, purpose, location and load pattern, which will provide basic data that can suggest optimal design guidelines for hybrid systems.

Acknowledgments: This work was supported by the New & Renewable Energy Core Technology Program of the Korea Institute of Energy Technology Evaluation and Planning (KETEP), granted financial resource from the Ministry of Trade, Industry & Energy, Korea. (No. 20133030110900).

Author Contributions: All authors contributed equally to this work. All authors designed the simulations, discussed the results and implications and commented on the manuscript at all stages.

Conflicts of Interest: The authors declare no conflict of interest.

Nomenclature

Symbols

A	Area	m^2
C	Specific heat	kJ/kg °C
IAM	Incidence angle modifier	-
COP	Coefficient of performance	-
F_R	Heat removal factor of the collector	-
G	Radiation	kW/m^2
h	Heat transfer coefficient	W/m^2 °C
L	Pipe length	M
LCC	Life Cycle Cost	-
m	Mass flow rate	kg/s
P	Power consumption	W
P_m	Rated power of photovoltaic module	kW/m^2
P_A	Non-recurring cost	-
P_F	Recurring cost	-
Q_u	Rate at which energy is added to the flow stream by the collector	W
r	reflectance	-
S	Net absorbed solar radiation	W
SPF	Seasonal performance factor	-
T	temperature	°C
I	Inflation rate	-
U_T	Overall loss coefficient of the collector	W/m^2 °C
V	Volume flow rate	m^3/s

Greek letters

Tau(T)	Transmittance	-
Alpha(A)	Absorptance	-
rho(P)	Density	m^3/kg
eta(H)	Efficiency	-
Beta(B)	Damping factor of ground heat exchanger	-

Subscripts

C	Solar collector
GHE	Ground heat exchanger
υ	Balance of a unit volume in the storage
b	Beam radiation
d	Diffue radiation
n	Normal incidence
f	Circulating fluid
p	Heat balance per unit length of pipe
L	Overall
PV	Photovoltaic
abs	Absorber plate
T	Total (beam + diffuse)
amb	ambient

In	Inlet
Out	Outlet
Ground	ground
HP→B	The heat flow from heat pump to FCU
HP→ST	The heat flow from heat pump to storage
PVT→G	The heat flow from PVT to ground
PVT→ST	The heat flow from PVT to storage
PVT→B	The heat flow from PVT to FCU
HP→B	The heat flow from heat pump to FCU
ST→B	The heat flow from storage to FCU

References

1. Gard, H.P.; Adhikari, R.S. Transient Simulation of Conventional Hybrid Photovoltaic/Thermal (PV/T) Air Heating Collector. *Int. J. Energy Res.* **1998**, *22*, 547–562.
2. Takashima, T.; Tanaka, T.; Doi, T.; Kamoshida, J.; Tani, T.; Horigome, T. New proposal for photovoltaic-thermal solar energy utilization method. *Sol. Energy* **1994**, *52*, 241–245. [CrossRef]
3. Arpino, F.; Cortellessa, G.; Frattolillo, A. Experimental and Numerical Assessment of Photovoltaic Collectors Performance dependence on Frame Size and Installation Technique. *Sol. Energy* **2015**, *118*, 7–19. [CrossRef]
4. Badescu, V.; Landsberg, P.T.; De Vos, A. Application to Hybrid Solar Converters. *J. Appl. Phys.* **1997**, *81*, 15. [CrossRef]
5. Tripanagnostopoulos, Y.; Nousia, T.; Souliotis, M.; Yianoulis, P. Hybrid Photovoltaic/Thermal Solar Systems. *Sol. Energy* **2002**, *72*, 217–234. [CrossRef]
6. Mohsen, M.S.; Al-Ghandoor, A.; Al-Hinti, I. *Thermal Analysis of Compact Solar Water Heater under Local Climatic Conditions*; Elsevier Science B.V.: Amsterdam, The Netherlands, 2009; Volume 36, pp. 962–968.
7. Wang, H.; Qi, C. Performance Study of Underground Thermal Storage in a Solar-Ground Coupled Heat Pump System for Residential Buildings. *Energy Build.* **2008**, *40*, 1278–1286. [CrossRef]
8. Wang, X.; Zheng, M.; Zang, W.; Zhang, S.; Yang, T. Experimental Study of a Solar-Assisted Ground-Coupled Heat Pump System with Solar Seasonal Thermal Storage in Severe Cold Areas. *Energy Build.* **2010**, *42*, 2104–2110. [CrossRef]
9. Ozgener, O. Use of Solar Assisted Geothermal Heat Pump and Small Wind Turbine Systems for Heating Agricultural and Residential Buildings. *Energy* **2010**, *35*, 262–268. [CrossRef]
10. Chen, X.; Yang, H. Performance Analysis of a Proposed Solar Assisted Ground Coupled Heat Pump System. *Appl. Energy* **2012**, *97*, 888–896. [CrossRef]
11. Wang, E.; Fung, A.S.; Qi, C.; Leong, W.H. Performance prediction of a hybrid solar ground-source heat pump system. *Energy Build.* **2012**, *47*, 600–611. [CrossRef]
12. Yang, W.; Sun, L.; Chen, Y. Experimental Investigations of the Performance of a Solar-ground Source Heat pump system operated in heating modes. *Energy Build.* **2015**, *89*, 97–111. [CrossRef]
13. Hadorn, J.-C. IEA Solar and Heat Pump Systems Solar Heating and Cooling Task 44 & Heat Pump Program Annex 38. *Energy Procedia* **2012**, *30*, 125–133.
14. Solar Heating & Cooling Program International Energy Agency. Available online: www.iea-shc.org/task44 (accessed on 20 August 2017).
15. The Society of Air-Conditioning and Refrigerating Engineers of Korea. *Equipment Engineering Manual*; SAREK: Seoul, Korea, 2011; ISBN 9788995228289.
16. HellstrÄom, G. *Duct Ground Heat Storage Model Manual for Computer Code*; Department of Mathematical Physics, University of Lund: Lund, Sweden, 1989.
17. Duffie, J.A.; Beckman, W.A. *Solar Engineering of Thermal Processes*, 4th ed.; John Wiley & Sons, Inc.: Hoboken, NJ, USA, 2013.
18. Yu, M.G.; Nam, Y.; Yu, Y.; Seo, J. Study on the System Design of a Solar Assisted Ground Heat Pump System Using Dynamic Simulation. *Energies* **2016**, *9*, 291. [CrossRef]
19. Public Procurement Service in Korea, National Market Shopping Mall. Available online: http://shopping.g2b.go.kr/ (accessed on 20 August 2017).

20. Korea Energy Agency, Renewable Energy Center. Available online: http://www.knrec.or.kr/knrec/13/KNREC130110.asp?idx=1239 (accessed on 20 August 2017).
21. Beginning Farmers Center. Available online: http://www.returnfarm.com/web/rf/house/BD_list.do (accessed on 20 August 2017).
22. Korea Energy Agency. Available online: www.kemco.or.kr/web/kem_home_new/new_main.asp (accessed on 20 August 2017).
23. The Society of Air-conditioning and Refrigerating Engineers of Korea. *Society of Air-Conditioning and Refrigerating Engineers of Korea*; SAREK: Seoul, Korea, 2011; ISBM 978-89-952282-9-6.
24. Jeong, Y.-D.; Nam, Y. Performance Test of PVT-water System Considering Ambient Air and Circulating Water Temperature. *KIEAE J.* **2015**, *15*, 83–88. [CrossRef]
25. Kim, S.-M.; Chung, K.-S.; Kim, Y.-I. An Empirical Study of Hot Water Supply Patterns and Peak Time in Apartment Housing with District Heating System. *J. Energy Eng.* **2012**, *21*, 435–443. [CrossRef]